

AN INTRODUCTION TO QED & QCD

Dr Elena Accomando (University of Southampton)

Contents

Outline of Lectures	57
Textbooks	58
1 Relativistic Quantum Mechanics	59
1.1 The Klein-Gordon Equation	59
1.2 The Dirac Equation	60
2 Spin	63
2.1 Plane Wave Solutions of the Dirac Equation	64
2.2 Spin	65
2.3 Working with Dirac Spinors	66
2.4 Lorentz transformations on spinors	67
3 Quantum Electro-Dynamics	68
3.1 The QED Lagrangian.....	69
3.2 Feynman Rules	70
4 Calculation of Cross Sections	75
4.1 Phase Space Integrals	75
4.2 Return to Coulomb Scattering	76
4.3 The Coulomb Potential	77
4.4 e^+e^- Annihilation	78
5 Photon Scattering	79
5.1 Photon Polarisation	79
5.2 Compton Scattering.....	81
6 Strong interactions	83
6.1 QCD Lagrangian	83
6.2 Gauge Invariance	86
7 Renormalization	91
7.1 Dimensional regularisation and renormalisation scale	91
7.2 Running Coupling	93
Summary	97
Acknowledgments	97

<p style="text-align: center;">QED and QCD HEP Summer School 2016</p>

This course gives an introduction to the ingredients of gauge theories which are necessary to calculate cross sections for particular processes. The section headings are given below:

Outline of Lectures:

1. Relativistic Quantum Mechanics
2. Spin
3. Relativistic Electromagnetism
4. Coulomb Scattering, $e\mu \rightarrow e\mu$
5. Compton Scattering, $e\gamma \rightarrow e\gamma$
6. Colour
7. Renormalisation

This course runs in parallel with the Quantum Field Theory course, from which we will use some results. Some topics mentioned in this course will be covered in more detail in the Standard Model and Phenomenology courses next week.

Textbooks:

These notes are intended to be self-contained, but only provide a short introduction to a complex and fascinating topic. You may find the following textbooks useful:

1. Aitchison and Hey, *Gauge Theories in Particle Physics*, CRC Press.
2. Halzen and Martin, *Quarks and Leptons*, Wiley.
3. Peskin and Schröder, *An Introduction to Quantum Field Theory*, ABP.
4. Ryder, *Quantum Field Theory*, CUP.
5. Srednicki, *Quantum Field Theory*, CUP.
6. Schwartz, *Quantum Field Theory and the Standard Model*, CUP.

The first two are more practical and closer to the spirit of this course while the other contain many more mathematical details. The last one is very recent. If you are particularly interested in (or confused by) a particular topic, I encourage you to take a look at it. If there are other textbooks which you find particularly helpful, please tell me and I will update the list.

These notes are based heavily on the content of previous versions of this course, in particular the 2013 version by Jennifer Smillie. Throughout, we will use “natural units” where $\hbar = c = 1$ and the metric signature $(+ - - -)$.

Please email any comments, questions or corrections to **a.banfi@sussex.ac.uk**.

Andrea Banfi
May 25, 2016

1 Relativistic Quantum Mechanics

In order to describe the dynamics of particles involved in high-energy collisions we must be able to combine the theory of phenomena occurring at the smallest scales, i.e. quantum mechanics, with the description of particles moving close to the speed of light, i.e. special relativity. To do this we must develop wave equations which are relativistically invariant (i.e. invariant under Lorentz transformations). In this section we will derive relativistic equations of motion for scalar particles (spin-0) and particles with spin-1/2.

1.1 The Klein-Gordon Equation

We start with the Hamiltonian for a particle in classical mechanics:

$$E = \frac{\mathbf{p}^2}{2m} + V(\mathbf{x}). \quad (1)$$

To convert this into a wave equation, we make the replacements $E \rightarrow i\partial_t$ and $\mathbf{p} \rightarrow -i\nabla$, so that a plane-wave solution

$$\phi(t, \mathbf{x}) \propto e^{-i(Et - \mathbf{p}\cdot\mathbf{x})} = e^{-ip\cdot x} \quad (2)$$

has the energy-momentum relation given in eq. (1). Applied to a general wavefunction ϕ , a linear superposition of plane waves, this gives

$$i\partial_t\phi(t, \mathbf{x}) = \left(-\frac{1}{2m}\nabla^2 + V(\mathbf{x})\right)\phi(t, \mathbf{x}) = H\phi(t, \mathbf{x}), \quad (3)$$

where H is the so-called Hamiltonian. We recognise this as the Schrödinger Equation, the cornerstone of Quantum Mechanics. From this form, we can deduce that eq. (3) cannot be relativistically invariant because time appears only through a first-order derivative on the left-hand side while space appears as a second-order derivative on the right-hand side. Yet we know that if we make a Lorentz transformation in the x direction for example, this would mix the x and t components and therefore they cannot have different rôles.

The problem with the Schrödinger Equation arose because we started from a non-relativistic energy-momentum relation. Let us then start from the relativistic equation for energy. For a particle with 4-momentum $p^\mu = (E, \mathbf{p})$ and mass m ,

$$E^2 = m^2 + \mathbf{p}^2. \quad (4)$$

Again we convert this to an operator equation by setting $p_\mu = i\partial_\mu$ so that the corresponding wave equation for an arbitrary scalar wavefunction $\phi(\mathbf{x}, t)$ gives

$$(\partial_t^2 - \nabla^2 + m^2)\phi(t, \mathbf{x}) = (\partial_\mu\partial^\mu + m^2)\phi(x) = (\square + m^2)\phi(x) = 0, \quad (5)$$

where we have introduced the four-vector $x^\mu = (t, \mathbf{x})$. This is the “Klein-Gordon equation” which is the equation of motion for a free scalar field. We can explicitly check that this is indeed Lorentz invariant. Under a Lorentz transformation

$$x^\mu \rightarrow x'^\mu = \Lambda^\mu_\nu x^\nu \quad \Rightarrow \quad \partial_\mu \rightarrow \partial'_\mu = (\Lambda^{-1})^\rho_\mu \partial_\rho, \quad (6)$$

The field ϕ is a scalar, i.e. it has the transformation property

$$\phi(x) \rightarrow \phi'(x') = \phi(\Lambda x) = \phi(x). \quad (7)$$

Therefore, in the primed system,

$$\begin{aligned} (\partial'_\mu \partial'^\mu + m^2) \phi'(x') &= [(\Lambda^{-1})^\rho_\mu \partial_\rho (\Lambda^{-1})^\sigma_\nu \partial_\sigma g^{\mu\nu} + m^2] \phi'(\Lambda x) \\ &= [\partial_\rho \partial_\sigma g^{\rho\sigma} + m^2] \phi(x) = 0, \end{aligned} \quad (8)$$

and the equation still holds.

1.2 The Dirac Equation

The Klein-Gordon equation admits negative-energy solutions, because the energy E appearing in the plane-wave in eq. (2) can have the two values $\pm \sqrt{\mathbf{p}^2 + m^2}$. Dirac sought to find an alternative relativistic equation which was linear in ∂_t like the Schrödinger equation (this was an attempt to solve the problem of negative-energy solutions to eq. (5) – in fact he didn’t solve this problem, but a different one). If the equation is linear in ∂_t , it must also be linear in ∇ if it is to be invariant under Lorentz transformations. We therefore start with the general form

$$i\partial_t \psi(t, \mathbf{x}) = (-i\boldsymbol{\alpha} \cdot \nabla + \beta m) \psi(t, \mathbf{x}). \quad (9)$$

Dirac also required that the solutions of his equation would be a solution of the Klein-Gordon equation as well, or equivalently, the energy relation eq. (4) was the correct energy-momentum relation for plane wave solutions $e^{-ip \cdot x}$ of the Dirac equation. To see what constraints this imposes, we must square eq. (9):

$$\begin{aligned} -\partial_t^2 \psi(t, \mathbf{x}) &= i\partial_t (-i\boldsymbol{\alpha} \cdot \nabla + \beta m) \psi(t, \mathbf{x}) \\ &= (-i\boldsymbol{\alpha} \cdot \nabla + \beta m)^2 \psi(t, \mathbf{x}) \\ &= [-\alpha^i \alpha^j \nabla^i \nabla^j - i(\beta \alpha^i + \alpha^i \beta) m \nabla^i + \beta^2 m^2] \psi(t, \mathbf{x}). \end{aligned} \quad (10)$$

However, the Klein-Gordon equation requires that the right-hand side is equal to $[-\nabla^2 + m^2] \psi(t, \mathbf{x})$ and therefore $\boldsymbol{\alpha}$ and β must satisfy

$$\alpha^i \alpha^j + \alpha^j \alpha^i = \{\alpha^i, \alpha^j\} = 2\delta^{ij}, \quad \beta \alpha^i + \alpha^i \beta = \{\alpha^i, \beta\} = 0, \quad \beta^2 = 1. \quad (11)$$

If α^i and β are just numbers, these equations cannot be solved. Dirac solved them by instead taking α^i and β to be $n \times n$ matrices, and $\psi(t, \mathbf{x})$ to be a column vector. Even now, the solution is not immediate. One can show that the conditions in eq. (11) require

$$\text{Tr } \alpha^i = 0 = \text{Tr } \beta, \quad (12)$$

and further that the eigenvalues of the above matrices are ± 1 . This in turn means that n must be even (do you understand why?). In 2-dimensions, there are still not enough linearly independent matrices to satisfy eq. (11). There do exist solutions in four dimensions. One such solution is

$$\boldsymbol{\alpha} = \begin{pmatrix} 0 & \boldsymbol{\sigma} \\ \boldsymbol{\sigma} & 0 \end{pmatrix}, \quad \beta = \begin{pmatrix} \mathbb{1}_2 & 0 \\ 0 & -\mathbb{1}_2 \end{pmatrix}, \quad (13)$$

where $\boldsymbol{\sigma}$ are the usual Pauli matrices and $\mathbb{1}_2$ represents the 2×2 identity matrix. Now we have formed an equation which may be thought of as a square-root of the Klein-Gordon equation, but which is not obviously Lorentz invariant. To show that, we first define the new matrices

$$\gamma^0 = \beta, \quad \boldsymbol{\gamma} = \beta \boldsymbol{\alpha}. \quad (14)$$

Then we form $\gamma^\mu = (\gamma^0, \boldsymbol{\gamma})$ where the μ is a Lorentz index. Each component is a 4×4 matrix. In terms of the γ -matrices, one can write the conditions in eq. (11) in a Lorentz covariant form

$$\{\gamma^\mu, \gamma^\nu\} = \gamma^\mu \gamma^\nu + \gamma^\nu \gamma^\mu = 2g^{\mu\nu}. \quad (15)$$

This is an example of a Clifford algebra. Any matrices satisfying this condition in eq. (15) may be used to construct the Dirac equation. The representation in eqs. (13) and (14) is just one example, known as the Dirac representation. Note, for example, that any other matrices satisfying

$$\alpha'_i = \mathbf{U} \alpha_i \mathbf{U}^{-1}, \quad \text{and} \quad \beta' = \mathbf{U} \beta \mathbf{U}^{-1}, \quad (16)$$

where \mathbf{U} is a unitary matrix, will also be suitable.

Multiplying through by γ^0 , we may rewrite the eq. (9) in a covariant form as

$$(i\gamma^\mu \partial_\mu - m\mathbb{1}_4)\psi(t, \mathbf{x}) = (i\not{\partial} - m)\psi(x) = 0, \quad (17)$$

where $\not{\partial}$, a vector with a slash, is a short-hand notation for $\gamma^\mu a_\mu$. The equation above is known as the Dirac equation. In momentum space, i.e. after a Fourier transformation, $\partial_\mu \rightarrow -ip_\mu$, and the Dirac equation becomes

$$(\gamma^\mu p_\mu - m\mathbb{1}_4)\tilde{\psi}(p) = (\not{p} - m)\tilde{\psi}(p) = 0, \quad (18)$$

where $\tilde{\psi}(p)$ is the Fourier transform of a solution of the Dirac equation $\psi(x)$.

We mentioned in passing that $\psi(t, \mathbf{x})$ is a column vector rather than a scalar. This means that it contains more than one degree of freedom. Dirac exploited this property to interpret his equation as the wave equation for spin-1/2 particles, fermions, which can be either spin-up or spin-down. The column vector ψ is known as a Dirac spinor.

Comparing eq. (9) to the Schrödinger equation in eq. (3) gives the Hamiltonian for a free spin-1/2 particle:

$$H_{\text{Dirac}} = -i\boldsymbol{\alpha} \cdot \nabla + \beta m. \quad (19)$$

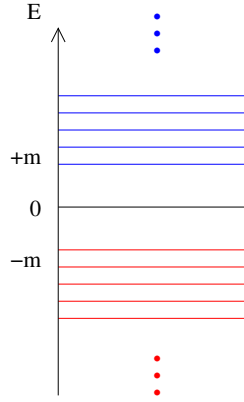


Figure 1: The energy levels in the Dirac sea picture. They must satisfy $|E| > m$, but negative-energy states are allowed. The vacuum is the state in which all negative-energy levels are filled.

The trace of the Hamiltonian gives the sum of the energy eigenvalues. The condition that the matrices α and β are traceless therefore means that the eigenvalues of H_{Dirac} must sum to zero. Therefore, like the Klein-Gordon equation, also the Dirac equation has negative-energy solutions.

Dirac himself proposed a solution for this problem which became known as the “Dirac sea”. He accepted the existence of negative-energy states, but took the vacuum as the state in which all these states are filled, see fig. 1. There is a conceptual problem with this in that the vacuum has infinite negative charge and energy. However, any observation relies only on energy differences, so this picture can give an acceptable theory.

As the negative-energy states are already full, the Pauli exclusion principle forbids any positive-energy electron to fall into one of the negative-energy states. If instead energy is supplied, an electron is excited from a negative-energy state to a positive-energy state and an “electron-hole” pair is created. The absence of the negative-energy electron, the hole, is interpreted as the presence of a state with positive energy and positive charge, i.e. a positron. Dirac predicted the existence of the positron in 1927 and this particle was discovered five years later.

However, Dirac’s argument only holds for spin-1/2 particles which obey the Pauli exclusion principle. A consistent solution for all particles is provided by Quantum Field Theory in a picture developed by Feynman and Stückelberg, in which positive-energy particles travel only *forward* in time, whereas negative-energy particles travel only *backwards* in time. In this way, a negative-energy particle with momentum p^μ , travelling backward in time, is re-interpreted as a positive energy anti-particle with momentum $-p^\mu$ travelling forward in time. Let us see how this picture naturally arises by considering two processes, the scattering $e^- \mu^- \rightarrow e^- \mu^-$, and Compton scattering $e^- \gamma \rightarrow e^- \gamma$. In non-relativistic quantum mechanics, the scattering $e^- \mu^- \rightarrow e^- \mu^-$ corresponds to the scattering of an electron from an external Coulomb potential. This is represented on the left-hand side of fig. 2. The horizontal axis represents the time at which a give elementary process occurs.

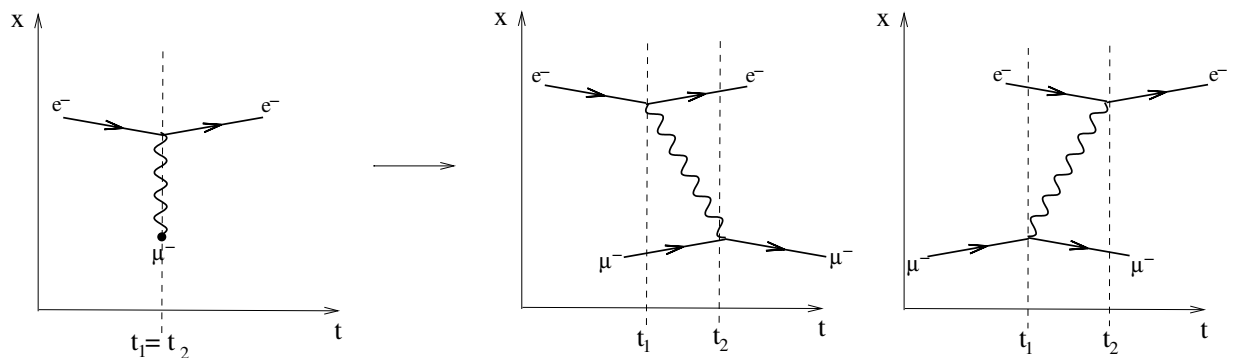


Figure 2: A pictorial representation of the scattering $e^- \mu^- \rightarrow e^- \mu^-$ in non-relativistic quantum mechanics (left) and in Quantum Field Theory (right).

In non-relativistic quantum mechanics, scattering happens instantaneously, so that the time t_1 at which a photon is emitted by the incoming electron coincides with the time t_2 in which it is absorbed by a muon, which stays at rest as a source of a static potential. In quantum field theory the scattering cannot occur instantaneously, because we need to take into account the fact that the photon mediating the scattering travels at the speed of light. The corresponding scattering amplitude is given by the sum of the contributions of the two diagrams on the right-hand side of fig. 2. It is clear that, in the limit in which c can be taken to be infinite, the two diagrams coincide and give the non-relativistic contribution. From the point of view of the electron, the first diagram can be interpreted as the emission of a positive-energy photon at $t = t_1$ that travels forward in time, and is later absorbed by a muon at $t = t_2$. The second diagram has an awkward interpretation from the point of view of the electron, because it corresponds to the emission of a negative-energy photon at $t = t_2$ that travels *backwards* in time. However, the graph makes perfectly sense if one considers that it is the muon that emits a photon a time t_1 , which is later reabsorbed by the electron at a time t_2 . A similar interpretation can be applied to the Compton scattering diagrams in Fig. 3, and clarifies the Feynman and Stückelberg interpretation of negative-energy states. In the left diagram, an electron emits a photon at time t_1 and later, at time t_2 absorbs another one. In the right-hand diagram it appears as if an electron emits a photon and then travels backwards in time to absorb another photon. Feynman and Stückelberg reasoned instead that the incoming photon split into an electron-positron pair and then at a later time, the positron annihilates the other electron, emitting a photon.

2 Spin

In the previous section, we introduced a Dirac spinor as a solution to the Dirac equation in the form of a column vector. In this section, we will discuss the explicit form of the solutions to the Dirac equation, and verify that they indeed correspond to the wave functions for particles with spin-1/2.

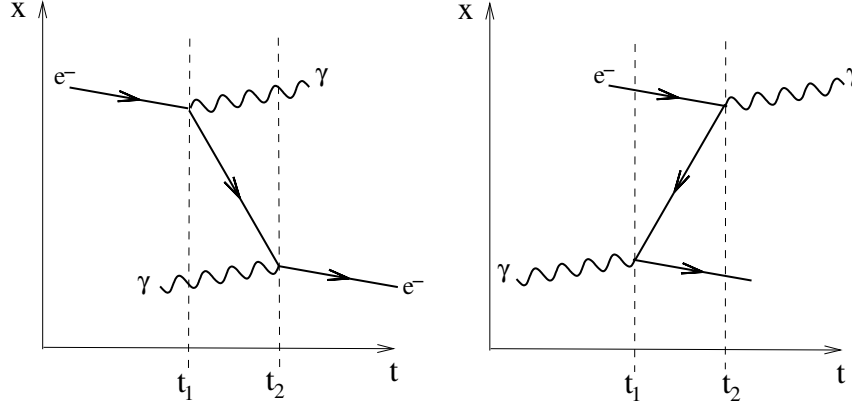


Figure 3: Diagrams illustrating the Feynman-Stückelberg interpretation of negative-energy particles, which correspond to those travelling backwards in time, as in the right-hand diagram. They interpreted a negative-energy particle travelling backwards as a positive-energy anti-particle travelling forwards in time, see text.

2.1 Plane-Wave Solutions of the Dirac Equation

We begin by seeking plane-wave solutions to the Dirac Equation. Given the 2×2 block nature of the γ -matrices, we will start with the form

$$\psi(x) = \begin{pmatrix} \chi(\mathbf{p}) \\ \phi(\mathbf{p}) \end{pmatrix} e^{-ip \cdot x}, \quad (20)$$

where χ and ϕ are two-component spinors. Substituting this into eq. (18) and using eqs. (13) and (14), we find

$$p^0 \begin{pmatrix} \chi \\ \phi \end{pmatrix} = \begin{pmatrix} m & \boldsymbol{\sigma} \cdot \mathbf{p} \\ \boldsymbol{\sigma} \cdot \mathbf{p} & -m \end{pmatrix} \begin{pmatrix} \chi \\ \phi \end{pmatrix}, \quad (21)$$

or equivalently

$$\begin{aligned} (\boldsymbol{\sigma} \cdot \mathbf{p}) \phi &= (p^0 - m)\chi \\ (\boldsymbol{\sigma} \cdot \mathbf{p}) \chi &= (p^0 + m)\phi. \end{aligned} \quad (22)$$

From the identity $(\boldsymbol{\sigma} \cdot \mathbf{p})^2 = \mathbf{p}^2$, these equations are only consistent for particles with $p^0 = \pm\sqrt{\mathbf{p}^2 + m^2}$ (consistent with having solutions of the Klein-Gordon equation).

For a massive fermion at rest ($\mathbf{p} = 0$), we have

$$p^0 \chi = m\chi \quad \text{and} \quad p^0 \phi = -m\phi. \quad (23)$$

Positive-energy solutions $\psi_+^{\mathbf{p}=0}$ must therefore have $\phi = 0$ and negative energy solutions $\psi_-^{\mathbf{p}=0}$ have $\chi = 0$, as follows:

$$\psi_+^{\mathbf{p}=0} = \begin{pmatrix} \chi \\ 0 \end{pmatrix} e^{-imt}, \quad \text{and} \quad \psi_-^{\mathbf{p}=0} = \begin{pmatrix} 0 \\ \phi \end{pmatrix} e^{imt}. \quad (24)$$

For particles which are not at rest ($\mathbf{p} \neq 0$), the solution is then dictated by eq. (22), with the requirement that it reduces to eq. (24) for $\mathbf{p} = 0$. For positive-energy solutions, we therefore write

$$\psi_+(x) = \mathcal{N} \left(\begin{array}{c} \chi_r \\ \frac{\boldsymbol{\sigma} \cdot \mathbf{p}}{E+m} \chi_r \end{array} \right) e^{-ip \cdot x} \equiv u_r(\mathbf{p}) e^{-ip \cdot x}, \quad p^0 = E \equiv \sqrt{\mathbf{p}^2 + m^2}, \quad (25)$$

where $r = 1, 2$ and \mathcal{N} is a normalisation conventionally chosen such that $u_r^\dagger(\mathbf{p}) u_s(\mathbf{p}) = 2E \delta^{rs}$, which gives $\mathcal{N} = \sqrt{E+m}$. The spinors χ_1 and χ_2 cover the two (spin) degrees of freedom:

$$\chi_1 = \begin{pmatrix} 1 \\ 0 \end{pmatrix}, \quad \text{and} \quad \chi_2 = \begin{pmatrix} 0 \\ 1 \end{pmatrix}. \quad (26)$$

Similarly, negative-energy solutions are conventionally written as

$$\psi_-(x) = \mathcal{N} \left(\begin{array}{c} \frac{\boldsymbol{\sigma} \cdot \mathbf{p}}{E+m} \phi_r \\ \phi_r \end{array} \right) e^{ip \cdot x} \equiv v_r(\mathbf{p}) e^{ip \cdot x}, \quad p^0 = E, \quad (27)$$

with the spinors ϕ_1 and ϕ_2 again covering the two (spin) degrees of freedom:

$$\phi_1 = \begin{pmatrix} 1 \\ 0 \end{pmatrix}, \quad \text{and} \quad \phi_2 = \begin{pmatrix} 0 \\ 1 \end{pmatrix}. \quad (28)$$

The spinors $u(\mathbf{p})$ and $v(\mathbf{p})$ therefore represent particle and anti-particle solutions with momentum \mathbf{p} and energy $E = \sqrt{\mathbf{p}^2 + m^2}$.

2.2 Spin

Each Dirac spinor has two linearly independent solutions which we stated earlier corresponded to the two possible spin states of a fermion. In this subsection we will define the corresponding spin operator. If we again consider a particle at rest we have

$$u_1 = \begin{pmatrix} 1 \\ 0 \\ 0 \\ 0 \end{pmatrix}, \quad \text{and} \quad u_2 = \begin{pmatrix} 0 \\ 1 \\ 0 \\ 0 \end{pmatrix}. \quad (29)$$

These have eigen-values $\pm \frac{1}{2}$ under the matrix

$$\frac{1}{2} \begin{pmatrix} \sigma_z & 0 \\ 0 & 0 \end{pmatrix}. \quad (30)$$

One can repeat the same thing for anti-particles and generalise to all the Pauli matrices to deduce the ‘‘spin operator’’

$$\mathbf{S} = \frac{1}{2} \begin{pmatrix} \boldsymbol{\sigma} & 0 \\ 0 & \boldsymbol{\sigma} \end{pmatrix}. \quad (31)$$

You can check explicitly that $\mathbf{S}^2 = \frac{3}{4}\mathbf{1}_4$, as we would expect. Therefore, for particles at rest, $\mathbf{p} = 0$, the top two components of ψ_+ describe fermions with $S_z = +1/2$ (spin up) and $S_z = -1/2$ (spin down) respectively.

In case of a general \mathbf{p} one can consider the projection of the spin-operator along the direction of motion of a particle, i.e. $\mathbf{p}/|\mathbf{p}|$. This gives the helicity operator, $h(\mathbf{p})$

$$h(\mathbf{p}) = \begin{pmatrix} \frac{\boldsymbol{\sigma} \cdot \mathbf{p}}{|\mathbf{p}|} & \mathbf{0} \\ \mathbf{0} & \frac{\boldsymbol{\sigma} \cdot \mathbf{p}}{|\mathbf{p}|} \end{pmatrix}. \quad (32)$$

This operator satisfies $h(\mathbf{p})^2 = 1$, and hence its eigenvalues are ± 1 .

2.3 Working with Dirac Spinors

So far we have discussed Dirac spinors, ψ , describing spin-1/2 particles and how Dirac used his equation to predict anti-particles. To generate an equation for anti-particles, we first take the Hermitian conjugate of the Dirac equation and find

$$\psi^\dagger(-i\gamma^0 \overleftarrow{\partial}_0 + i\gamma^i \overleftarrow{\partial}_i - m) = 0, \quad (33)$$

where the arrows over the derivatives just mean they act on the left, and we have used the fact that $\gamma^{0\dagger} = \gamma^0$ and $\gamma^{i\dagger} = -\gamma^i$. All matrices have to be written on the right because they are multiplying matrices and ψ^\dagger is a row-vector. The above equation does not seem Lorentz covariant. This can be rectified by multiplying the equation by γ^0 on the right-hand side and using $[\gamma^0, \gamma^i] = 0$. Then we have

$$(\psi^\dagger \gamma^0)(-i\overleftarrow{\not{\partial}} - m) = 0, \quad \text{or} \quad \overline{\psi}(i\overleftarrow{\not{\partial}} + m) = 0. \quad (34)$$

The interpretation of the above equation is that the field $\overline{\psi} \equiv \psi^\dagger \gamma^0$ represents an anti-particle.

By construction, the spinors $u(\mathbf{p})$ and $v(\mathbf{p})$ satisfy their respective Dirac equations in momentum space:

$$(\not{p} - m)u(\mathbf{p}) = 0, \quad (\not{p} + m)v(\mathbf{p}) = 0. \quad (35)$$

They also satisfy a number of relations which will prove very useful in calculations of scattering amplitudes. Firstly, they are orthonormal:

$$\begin{aligned} \overline{u}_r(\mathbf{p})u_s(\mathbf{p}) &= 2m \delta^{rs} = -\overline{v}_r(\mathbf{p})v_s(\mathbf{p}), \\ \overline{u}_r(\mathbf{p})v_s(\mathbf{p}) &= 0 = -\overline{v}_r(\mathbf{p})u_s(\mathbf{p}). \end{aligned} \quad (36)$$

If instead one takes the outer product of spinor and anti-spinor, they also satisfy the following completeness relations:

$$\sum_{r=1}^2 u_r(\mathbf{p})\overline{u}_r(\mathbf{p}) = (\not{p} + m) \quad \text{and} \quad \sum_{r=1}^2 v_r(\mathbf{p})\overline{v}_r(\mathbf{p}) = (\not{p} - m). \quad (37)$$

These relations can be checked explicitly (see problem sheet).

2.4 Lorentz transformations on spinors

Let us consider the Lorentz transformation of eq. (6). The field ψ has the transformation property

$$\psi(x) \rightarrow \psi'(x') = \psi'(\Lambda x) = S(\Lambda)\psi(x) \quad \Rightarrow \quad \bar{\psi}(x) \rightarrow \bar{\psi}'(x') = \bar{\psi}(x)\gamma^0 S^\dagger(\Lambda)\gamma^0, \quad (38)$$

with $S(\Lambda)$ a suitable 4×4 matrix. Its explicit form is derived by imposing that the Dirac equation is Lorentz invariant:

$$(i\partial'_\mu \gamma^\mu - m) \psi'(x') = (i(\Lambda^{-1})^\nu_\mu \partial_\nu \gamma^\mu - m) S(\Lambda)\psi(x). \quad (39)$$

Imposing that $S(\Lambda)$ satisfies

$$\gamma^\mu S(\Lambda) = S(\Lambda)\Lambda^\mu_\rho \gamma^\rho, \quad (40)$$

we obtain

$$\begin{aligned} (i\partial'_\mu \gamma^\mu - m) \psi'(x') &= S(\Lambda) [i(\Lambda^{-1})^\nu_\mu \Lambda^\mu_\rho \partial_\nu \gamma^\rho - m] \psi(x) \\ &= S(\Lambda)(i\partial_\nu \gamma^\nu - m)\psi(x) = 0, \end{aligned} \quad (41)$$

so that $\psi'(x')$ is a solution of the transformed Dirac equation, provided $\psi(x)$ is a solution of the original one.

Eq. (40) is enough to construct the matrices $S(\Lambda)$. By direct inspection one observes that

$$S^\dagger(\Lambda) = \gamma^0 S^{-1}(\Lambda)\gamma^0 \quad \Rightarrow \quad \bar{\psi}'(x') = S^{-1}(\Lambda)\bar{\psi}(x). \quad (42)$$

The fact that $S^{-1}(\Lambda) \neq S^\dagger(\Lambda)$ is not surprising, and is due to the fact that the Lorentz group is non-compact, and therefore it does not admit unitary finite-dimensional representations.

One can construct bi-linear products $\bar{\psi}\Gamma\psi$, with Γ a 4×4 matrix. We now show that Γ can be decomposed into a set of bi-linears, each having a definite transformation property under the Lorentz group. Since Γ is 4×4 matrix, we expect to find 16 such bi-linear products, constructed out of linearly independent matrices. Already we can find 5 such bi-linears:

$$\begin{aligned} \bar{\psi}\psi &\rightarrow \bar{\psi}S^{-1}(\Lambda)S(\Lambda)\psi = \bar{\psi}\psi && \text{(scalar)}, \\ \bar{\psi}\gamma^\mu\psi &\rightarrow \bar{\psi}S^{-1}(\Lambda)\gamma^\mu S(\Lambda)\psi = \Lambda^\mu_\nu (\bar{\psi}\gamma^\nu\psi) && \text{(vector)}, \end{aligned} \quad (43)$$

We can construct 6 more matrices by considering

$$\Sigma^{\mu\nu} = \frac{i}{4}[\gamma^\mu, \gamma^\nu]. \quad (44)$$

Note that $\gamma^\mu\gamma^\nu$ is not linearly independent from the previous matrices because $\{\gamma^\mu\gamma^\nu\} = 2g^{\mu\nu}\mathbb{1}$. This gives

$$\bar{\psi}\Sigma^{\mu\nu}\psi \rightarrow \bar{\psi}S^{-1}(\Lambda)\frac{i}{4}[\gamma^\mu, \gamma^\nu]S(\Lambda)\psi = \Lambda^\mu_\rho \Lambda^\nu_\sigma (\bar{\psi}\Sigma^{\rho\sigma}\psi) \quad \text{(tensor)}. \quad (45)$$

In addition to the four γ -matrices, we can construct their product which is conventionally known as γ^5 :

$$\gamma^5 \equiv i\gamma^0\gamma^1\gamma^2\gamma^3 = \frac{i}{4!} \epsilon_{\mu\nu\rho\sigma} \gamma^\mu \gamma^\nu \gamma^\rho \gamma^\sigma = \begin{pmatrix} -\mathbf{1}_2 & 0 \\ 0 & \mathbf{1}_2 \end{pmatrix}, \quad (46)$$

which satisfies

$$(\gamma^5)^2 = \mathbf{1}, \quad \{\gamma^5, \gamma^\mu\} = 0, \quad (\gamma^5)^\dagger = \gamma^5. \quad (47)$$

The factor of i is to make then matrix Hermitian. Using γ^5 , we can construct 5 more bi-linears

$$\begin{aligned} \bar{\psi} \gamma^5 \psi &\rightarrow \bar{\psi} S^{-1}(\Lambda) i \epsilon_{\mu\nu\rho\sigma} \gamma^\mu \gamma^\nu \gamma^\rho \gamma^\sigma S(\Lambda) \psi \\ &= i \epsilon_{\mu\nu\rho\sigma} \Lambda_\alpha^\mu \Lambda_\beta^\nu \Lambda_\gamma^\rho \Lambda_\delta^\sigma (\bar{\psi} \gamma^\alpha \gamma^\beta \gamma^\gamma \gamma^\delta \psi) \\ &= \det(\Lambda) \bar{\psi} i \epsilon_{\alpha\beta\gamma\delta} \gamma^\alpha \gamma^\beta \gamma^\gamma \gamma^\delta \psi = \det(\Lambda) \bar{\psi} \gamma^5 \psi \quad (\text{pseudo-scalar}), \\ \bar{\psi} \gamma^5 \gamma^\mu \psi &\rightarrow \det(\Lambda) \Lambda_\nu^\mu (\bar{\psi} \gamma^5 \gamma^\nu \psi) \quad (\text{pseudo-vector}). \end{aligned} \quad (48)$$

We have then found a set of 16 linearly independent matrices (check that they are linearly independent!)

$$\mathbf{1}, \gamma^5, \gamma^\mu, \gamma^\mu \gamma^5, \Sigma^{\mu\nu} = \frac{i}{4} [\gamma^\mu, \gamma^\nu], \quad (49)$$

so that any bi-linear $\bar{\psi} \Gamma \psi$ can be written as a sum of terms with definite transformation properties, i.e. transforming in a clear way as a scalar, pseudo-scalar, vector, pseudo-vector and tensor. (This is why the Feynman rule for a pseudo-scalar interacting with a particle-anti-particle pair has a γ^5 for example.)

The most common use of γ^5 is in the projectors $P_L = (1 - \gamma^5)/2$ and $P_R = (1 + \gamma^5)/2$. You can check explicitly that these behave like projectors (ie. $P^2 = P$ and $P_L P_R = 0$). When these act upon a Dirac spinor they project out either the component with “left-handed” *chirality* or with “right-handed” chirality. These projectors therefore appear when considering weak interactions, for example, as W bosons only couple to left-handed particles. One has to take care when defining the handedness of antiparticles because

$$\bar{\psi}_L = \psi_L^\dagger \gamma^0 = \psi^\dagger P_L \gamma^0 = \psi^\dagger \gamma^0 P_R = \bar{\psi} P_R. \quad (50)$$

A left-handed anti-particle appears with a right-handed projection operator next to it and vice-versa.

3 Quantum Electro-Dynamics

In this section, we will develop the theory of quantum electro-dynamics (QED) which describes the interaction between electrically charged fermions and a vector field (the photon A^μ).

3.1 The QED Lagrangian

In this course, we have so far considered spin-0 and spin-1/2 particles. We will postpone a detailed discussion of spin-1 particles until section 5.1. For the time being, we start from the Maxwell's equations in the vacuum in relativistic notation:

$$\partial_\mu F^{\mu\nu} = J^\nu, \quad \text{where} \quad F^{\mu\nu} = \partial^\mu A^\nu - \partial^\nu A^\mu, \quad (51)$$

and J^ν is a conserved current, i.e. satisfying $\partial_\nu J^\nu = 0$. Maxwell's equations can be derived from the Lagrangian

$$\mathcal{L} = \mathcal{L}_{\text{em}} + \mathcal{L}_{\text{int}}, \quad \mathcal{L}_{\text{em}} = -\frac{1}{4}F^{\mu\nu}F_{\mu\nu}, \quad \mathcal{L}_{\text{int}} = -J^\mu A_\mu, \quad (52)$$

by applying Euler-Lagrange equations

$$\partial_\mu \frac{\partial \mathcal{L}}{\partial(\partial_\mu A_\nu)} - \frac{\partial \mathcal{L}}{\partial A_\nu} = -\partial_\mu F^{\mu\nu} + J^\nu = 0. \quad (53)$$

The Dirac equation for ψ and its equivalent for $\bar{\psi}$ can be derived from the Lagrangian

$$\mathcal{L}_{\text{Dirac}} = \bar{\psi}(i\gamma^\mu \partial_\mu - m)\psi. \quad (54)$$

The starting point for the QED Lagrangian is then the sum of \mathcal{L}_{em} and $\mathcal{L}_{\text{Dirac}}$. However, in order to make the theory describe interactions, we must include a term which couples A^μ to ψ and $\bar{\psi}$. If we wish Maxwell's equation to be valid, this term has to be of the form $\mathcal{L}_{\text{int}} = -J^\mu A_\mu$, with J^μ a conserved vector current. We then observe that the vector current $J^\mu = \bar{\psi} \gamma^\mu \psi$ is conserved if ψ is a solution of Dirac equation. In fact

$$\partial_\mu J^\mu = \bar{\psi} \overleftarrow{\not{\partial}} \psi + \bar{\psi} (\partial \psi) = (-m\bar{\psi}) + \bar{\psi} (m\psi) = 0. \quad (55)$$

Therefore, a good candidate for the electromagnetic current describing an electron of charge $-e$ is

$$J^\mu = -e \bar{\psi} \gamma^\mu \psi, \quad (56)$$

where $-e$ multiplies the vector current so as to be sure that the resulting Coulomb potential arising from the solution of the static Maxwell's equations is the expected one. Using the above current, we obtain:

$$\mathcal{L} = \mathcal{L}_{\text{em}} + \mathcal{L}_{\text{Dirac}} + \mathcal{L}_{\text{int}} = -\frac{1}{4}F^{\mu\nu}F_{\mu\nu} + \bar{\psi}(i\not{\partial} - m)\psi + e\bar{\psi} \gamma^\mu \psi A_\mu. \quad (57)$$

Notice that \mathcal{L} is invariant with respect to the "gauge" transformations

$$\psi(x) \rightarrow \psi'(x) = e^{-ie\alpha(x)}\psi(x), \quad A_\mu(x) \rightarrow A'_\mu(x) = A_\mu(x) + \partial_\mu \alpha(x). \quad (58)$$

Notice that the addition of the interaction term \mathcal{L}_{int} is equivalent to the replacement

$$\partial_\mu \rightarrow D_\mu = \partial_\mu - ieA_\mu. \quad (59)$$

This prescription is known as “minimal coupling” and automatically ensures that the Lagrangian is gauge invariant. The use of gauge invariance to introduce interactions will be covered in detail in the Standard Model course next week. This gives

$$\mathcal{L} = -\frac{1}{4}F^{\mu\nu}F_{\mu\nu} + \bar{\psi}(i\gamma^\mu(\partial_\mu + ieA_\mu)\psi). \quad (60)$$

The fact that \mathcal{L} is invariant under the gauge transformations in eq. (62) means that A^μ contains unphysical degrees of freedom. This is clear in view of the fact that a massless vector field contains two physical polarisations, whereas A^μ has four degrees of freedom. In order to eliminate this degeneracy, a “gauge-fixing” condition is imposed. A possible choice of a gauge condition is the so-called Coulomb gauge, in which $\nabla \cdot \mathbf{A} = 0$. Although this condition eliminates the two additional degrees of freedom, it breaks Lorentz covariance. A common choice that preserves Lorentz covariance is the Lorentz gauge:

$$\partial_\mu A^\mu = 0. \quad (61)$$

This corresponds to choosing the gauge parameter α such that $\square\alpha = -\partial_\mu A^\mu$ above. In this gauge, the Maxwell equations become $\square A^\nu = 0$.

Notice that the Lorentz gauge condition reduces the number of degrees of freedom in A from four to three. Even now though A^μ is not unique. A transformation of the form

$$A_\mu \rightarrow A'_\mu = A_\mu + \partial_\mu \chi, \quad \square\chi = 0, \quad (62)$$

will also leave the Lagrangian unchanged. At classical level we can eliminate the extra polarisation “by hand”, but at quantum level this cannot be done without giving up covariant canonical commutation rules. The way out, which can only be summarised, is to add a gauge-fixing Lagrangian \mathcal{L}_{gf} , so that the full QED Lagrangian becomes

$$\mathcal{L}_{\text{QED}} = \mathcal{L}_{\text{em}} + \mathcal{L}_{\text{Dirac}} + \mathcal{L}_{\text{int}} + \mathcal{L}_{\text{gf}}, \quad \mathcal{L}_{\text{gf}} = -\frac{1}{2\xi}(\partial_\mu A^\mu)^2. \quad (63)$$

Using this Lagrangian as a starting point, and an extra condition on physical states, only the two physical polarisations propagate on-shell. Notice that setting $\xi = 0$ corresponds to enforcing the Lorentz gauge condition $\partial_\mu A^\mu = 0$, otherwise the equations of motions give $\square\partial_\mu A^\nu = 0$, i.e. $\partial_\mu A^\nu$ is a free field.

3.2 Feynman Rules

Feynman developed a method of organising the calculation of scattering amplitudes in terms of diagrams. Starting from a set of vertices (or interactions), each corresponding to a term in the Lagrangian and a set of links (or propagators), you build every possible diagram corresponding to your initial and final state. Each piece comes with a “rule” and the combination of these give the scattering amplitude (actually $i\mathcal{M}$).

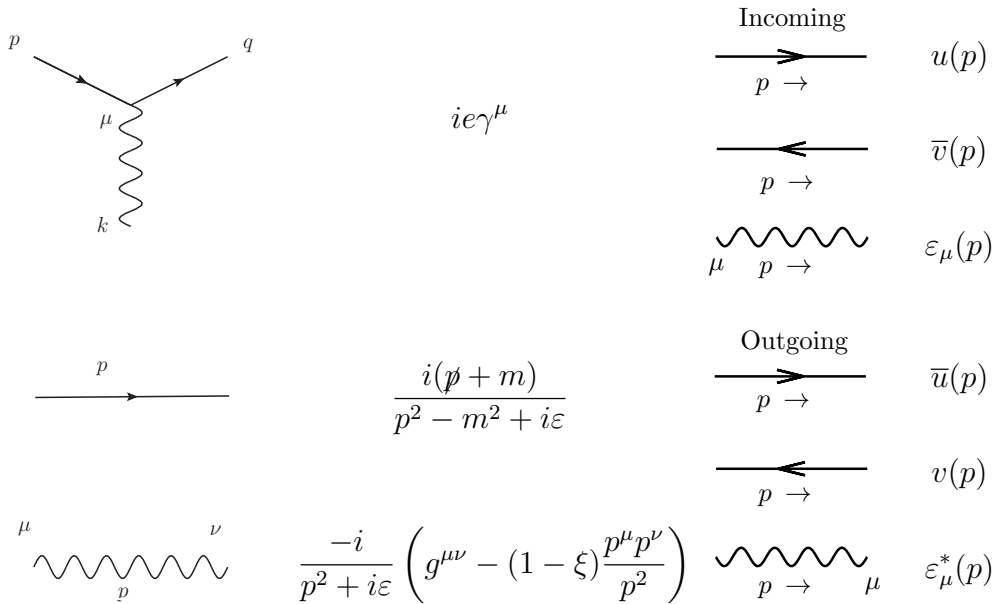


Figure 4: The Feynman rules for QED. Wavy lines represent a photon and straight lines represent any charged fermion. The arrow on the straight line tells you it is a particle or anti-particle depending on whether it is with or against momentum flow. The polarisation vectors $\epsilon_\mu(p)$ will be discussed in section 5.2.

In the quantum field theory course at this school, you learn how to derive the “Feynman rules” for scalar ϕ^4 theory. The principles are the same here so in this course we will state the Feynman rules for QED and learn how to work with them. The Feynman rules are shown in figure 4. The left-hand column represents internal parts of the diagram while the right-hand column gives the rules for external fermions and photons.

A few comments are necessary here:

1. Individual pieces of a Feynman diagram are a mixture of matrices, vectors, co-vectors and scalars. They do not commute. The final amplitude is a number and therefore you must follow each fermion line from a spinor (either outgoing particle or incoming anti-particle) through the series of matrices to finish on an anti-spinor (either incoming particle or out-going anti-particle). This corresponds to working backwards along the fermion line. We will see this in the examples which follow. Similarly, all Lorentz indices corresponding to photons have to be contracted.
2. The photon propagator term has a free parameter ξ . This is due to the gauge freedom we discussed in the previous section. It does not represent a physical degree of freedom and therefore any calculation of a physical observable will be independent of ξ . We will most commonly work in Feynman gauge $\xi = 1$.
3. The propagators come with factors of $i\epsilon$ in the denominator, otherwise they would have poles on the real axis and any integral over p would not be well-defined. The

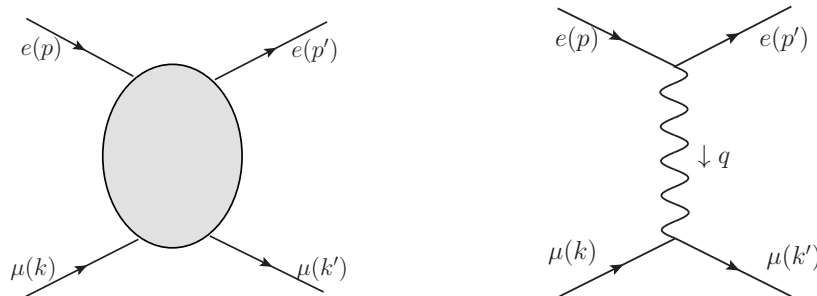


Figure 5: Building the leading-order Feynman diagram for Coulomb scattering. We start from the initial and final states on the left-hand side. The diagram on the right is the only way to connect these with up to two vertices.

factor of $i\varepsilon$ prescribes which direction to travel around the poles. This choice corresponds to the “Feynman prescription”, which ensures causality.

4. The interaction vertex contains only one flavour of fermion. We know that the emission of a photon does not change an electron to a quark for example.
5. There are additional factors of (-1) in the following scenarios:
 - (a) an anti-fermion line runs continuously from an initial to a final state;
 - (b) there is a closed fermion loop;
 - (c) between diagrams with identical fermions in the final state.

These arise from the anti-commutation properties of fermionic operators which is beyond the scope of this course. This sign can be important to get the relative phase between diagrams correct, as happens for instance in Bhabha scattering.

Examples: Coulomb Scattering

As a first example, we consider Coulomb scattering:

$$e(p) \mu(k) \rightarrow e(p') \mu(k'). \quad (64)$$

We start by drawing the external particles, see left-hand side of fig. 5. We now want to find all possible ways to connect these. There is no direct interaction between an electron and a muon but both interact with a photon, so a possible connected diagram is the one shown on the right-hand side. In fact, this is the only possible diagram with no more than two vertices. The number of vertices is directly related to the powers of the coupling e and therefore the diagram shown on the right is the leading-order (or tree-level) process.

If we consider $e(p) e(k) \rightarrow e(p') e(k')$ or $e^+(p) e^-(k) \rightarrow e^+(p') e^-(k')$ instead, there are two diagrams with two vertices, i.e. at $\mathcal{O}(e^2)$ (try this!). Both have to be added before squaring the amplitude to have the tree-level contribution to the cross section.

If we allow ourselves more than two vertices, there are many more diagrams we can draw. Since the number of external particles doesn't increase, these must contain closed loops and, therefore, they represent higher-loop processes. In this course, we will limit ourselves to tree-level processes. Loop-diagrams will be covered in the phenomenology course.

Now we will construct the tree-level amplitude for Coulomb scattering from the rules in Fig. 4. Keeping in mind the earlier warning about the ordering of matrices and spinors, we take each fermion line in turn. The electron line gives

$$\bar{u}(p') (ie\gamma^\mu) u(p). \quad (65)$$

In spin-space, this is co-vector–matrix–vector, which is a number. In Lorentz space it has one free index μ and is therefore a vector. Similarly, for the muon line we get

$$\bar{u}(k') (ie\gamma^\nu) u(k). \quad (66)$$

Lastly, for the propagator with momentum $q = p' - p = k - k'$ in Feynman gauge, we get

$$\frac{-ig_{\mu\nu}}{q^2 + i\varepsilon}, \quad (67)$$

so that the full amplitude is

$$i\mathcal{M} = ie^2 [\bar{u}(p') \gamma^\mu u(p)] \frac{g_{\mu\nu}}{q^2} [\bar{u}(k') \gamma^\nu u(k)]. \quad (68)$$

We will drop the $i\varepsilon$ from now on, as we will not need it in this example.

Just as in quantum mechanics, in order to compute the probability of this process happening, we must calculate $|\mathcal{M}|^2$. We will now add specific indices to label the spins, r, r', s, s' . In order to describe an unpolarised physical scattering process, we will average over initial-state spins and sum over final-state spins. This convention is represented by a bar as follows:

$$\begin{aligned} \overline{|\mathcal{M}|^2} &= \frac{1}{2} \sum_{r=1}^2 \frac{1}{2} \sum_{s=1}^2 \sum_{r'=1}^2 \sum_{s'=1}^2 |\mathcal{M}|^2 \\ &= \frac{1}{4} \frac{e^4}{(q^2)^2} \sum_{r,r'} [\bar{u}_{r'}(p') \gamma^\mu u_r(p)] [\bar{u}_{r'}(p') \gamma^\rho u_r(p)]^* \\ &\quad \times \sum_{s,s'} [\bar{u}_{s'}(k') \gamma_\mu u_s(k)] [\bar{u}_{s'}(k') \gamma_\rho u_s(k)]^*, \end{aligned} \quad (69)$$

where we have explicitly evaluated the metric contractions for brevity.

To evaluate the products in eq. (69) we will use the results from section 2.1. We will take the pieces corresponding to the electron line first. Since $[\bar{u}_{r'}(p') \gamma^\rho u_r(p)]^*$ is a number, its complex conjugate is its hermitian conjugate. Therefore

$$[\bar{u}_{r'}(p') \gamma^\rho u_r(p)]^* = u_r^\dagger(p) \gamma^{\rho\dagger} \gamma^{0\dagger} u_{r'}(p') = u_r^\dagger(p) \gamma^0 \gamma^\rho u_{r'}(p') = \bar{u}_r(p) \gamma^\rho u_{r'}(p'), \quad (70)$$

where we have used $\gamma^{\nu\dagger} = \gamma^0 \gamma^\nu \gamma^0$, which you showed on the problem sheet. We now use eq. (37) to find

$$\begin{aligned} \sum_{r,r'} [\bar{u}_{r'}(p') \gamma^\mu u_r(p)] [\bar{u}_{r'}(p') \gamma^\rho u_r(p)]^* &= \sum_{r,r'} \bar{u}_{r'}(p') \gamma^\mu u_r(p) \bar{u}_r(p) \gamma^\rho u_{r'}(p') \\ &= \sum_{r'} \bar{u}_{r'}(p') \gamma^\mu (\not{p} + m) \gamma^\rho u_{r'}(p'). \end{aligned} \quad (71)$$

We will use m for the electron mass and M for the muon mass. It is now useful to add a component index in spinor-space like you would do in normal linear algebra. Schematically we have

$$\sum_{r'} \bar{u}_{r'i} \Gamma_{ij} u_{r'j}, \quad (72)$$

where Γ represents the chain of γ -matrices in eq. (71). Now that we are explicitly labelling the components, we can swap the order of the terms to get

$$\sum_{r'} \Gamma_{ij} u_{r'j} \bar{u}_{r'i} = \Gamma_{ij} (\not{p}' + m)_{ji} = \text{Tr}(\gamma^\mu (\not{p}' + m) \gamma^\rho (\not{p}' + m)). \quad (73)$$

We could have anticipated that we would get a trace as we need to get a single number from a series of matrices. Working from the anti-commutation relations, one can readily show the following identities (see problem sheet):

$$\begin{aligned} \text{Tr}(\text{odd number of } \gamma \text{ matrices}) &= 0, & \text{Tr}(\gamma^\mu \gamma^\nu) &= 4g^{\mu\nu}, \\ \text{Tr}(\gamma^\mu \gamma^\nu \gamma^\rho \gamma^\sigma) &= 4(g^{\mu\nu} g^{\rho\sigma} - g^{\mu\rho} g^{\nu\sigma} + g^{\mu\sigma} g^{\nu\rho}). \end{aligned} \quad (74)$$

Therefore, eq. (73) equals

$$4p_\nu p'_\sigma (g^{\mu\nu} g^{\rho\sigma} - g^{\mu\rho} g^{\nu\sigma} + g^{\mu\sigma} g^{\nu\rho}) + 4m^2 g^{\mu\rho}. \quad (75)$$

The same series of steps gives

$$\sum_{s,s'} [\bar{u}_{s'}(k') \gamma_\mu u_s(k)] [\bar{u}_{s'}(k') \gamma_\rho u_s(k)]^* = 4k^\alpha k'^\beta (g_{\mu\alpha} g_{\rho\beta} - g_{\mu\rho} g_{\alpha\beta} + g_{\mu\beta} g_{\alpha\rho}) + 4M^2 g_{\mu\rho}. \quad (76)$$

Substituting these results into eq. (69) gives

$$|\overline{\mathcal{M}}|^2 = \frac{8e^4}{(q^2)^2} ((pk)(p'k') + (pk')(p'k) + 2m^2 M^2 - M^2(pp') - m^2(kk')). \quad (77)$$

We will now rewrite the invariants which appear in the above equation in terms of the centre-of-mass energy squared, s and the exchanged momentum-squared, $q^2 = t$. We have

$$\begin{aligned} 2(pk) &= (p+k)^2 - m^2 - M^2 = s - m^2 - M^2, & 2(p'k') &= s - m^2 - M^2 \\ 2(pp') &= -(p-p')^2 + 2m^2 = -q^2 + 2m^2, & 2(kk') &= -q^2 + 2M^2 \\ 2(pk') &= 2p \cdot (p+k-p') = s + q^2 - m^2 - M^2, & 2(p'k) &= s + q^2 - m^2 - M^2, \end{aligned} \quad (78)$$

which finally gives

$$|\overline{\mathcal{M}}|^2 = \frac{2e^4}{(q^2)^2} \left((s - m^2 - M^2)^2 + (s + q^2 - m^2 - M^2)^2 + 2q^2(m^2 + M^2) \right). \quad (79)$$

This expression can be further simplified by introducing the further invariant $u = (p - k')^2 = (p' - k)^2$:

$$|\overline{\mathcal{M}}|^2 = \frac{2e^4}{t^2} \left((s - m^2 - M^2)^2 + (u - m^2 - M^2)^2 + 2t(m^2 + M^2) \right). \quad (80)$$

The above equation gives the probability that the corresponding process occurs at a given point in phase space. In the next section, we will derive how to calculate a total cross section (or a total decay width) from amplitudes squared.

4 Calculation of Cross Sections

Ultimately it is not the amplitude we really want to calculate, but its integral over phase space to give the total cross section if it is a scattering process or the total decay width if it is a decay.

4.1 Phase Space Integrals

We must integrate over all the allowed phase space, which means all possible momentum configurations of the final-state particles. This result, divided by the flux of incoming particles, will give the total cross section.

In principle, we must integrate over over a 4-dimensional phase space for each particle f in the final state, but we must impose that each satisfies its on-shell condition $p_f^2 = m_f^2$. We therefore must have

$$\begin{aligned} \prod_f \int \frac{d^4 p_f}{(2\pi)^4} (2\pi) \delta(p_f^2 - m^2) \Theta(p_f^0) &= \prod_f \int \frac{d^4 p_f}{(2\pi)^4} (2\pi) \delta((p_f^0)^2 - \mathbf{p}_f^2 - m^2) \Theta(p_f^0) \\ &= \prod_f \int \frac{d^3 \mathbf{p}_f}{(2\pi)^3 (2E_f)}, \end{aligned} \quad (81)$$

where $E_f = \sqrt{\mathbf{p}_f^2 + m^2}$. Although the final expression explicitly separates the dependence on E and \mathbf{p} , it is still Lorentz invariant as the original expression is clearly Lorentz invariant. Eq. (81) is frequently referred to as the Lorentz Invariant Phase Space measure (LIPS). The factors of 2π correspond to the conventions used for momentum space integrations in QFT.

We now need to normalise this expression to the flux of incoming particles. This is done by multiplying by the flux factor, \mathcal{F} . For the scattering of two incoming particles, this is

usually written as

$$\mathcal{F} = \frac{1}{4E_a E_b |\mathbf{v}_a - \mathbf{v}_b|}, \quad (82)$$

where E_i and \mathbf{v}_i are the energy and velocity of each incoming particle.¹ A neater, equivalent form which explicitly demonstrates the Lorentz invariance of this quantity is

$$\mathcal{F} = \frac{1}{4\sqrt{(p_a p_b)^2 - m_a^2 m_b^2}}. \quad (83)$$

In the massless limit $s \gg m_1, m_2$, this simplifies to $\mathcal{F} \simeq 1/(2s)$. Finally, we must impose total conservation of momentum to find

$$\sigma = \mathcal{F} \left(\prod_f \int \frac{d^3 \mathbf{p}_f}{(2\pi)^3 (2E_f)} \right) |\overline{\mathcal{M}}|^2 (2\pi)^4 \delta^4 \left(\sum_f p_f - p_1 - p_2 \right). \quad (84)$$

If you wish to calculate a total decay width instead, the expression is very similar. The only difference is that the flux factor becomes

$$\mathcal{F} = \frac{1}{2M}, \quad (85)$$

where M is the mass of the decaying particle. The total decay width, Γ , is therefore given by

$$\Gamma = \frac{1}{2M} \left(\prod_f \int \frac{d^3 \mathbf{p}_f}{(2\pi)^3 (2E_f)} \right) |\overline{\mathcal{M}}|^2 (2\pi)^4 \delta^4 \left(\sum_f p_f - p_M \right). \quad (86)$$

4.2 Return to Coulomb Scattering

We may now calculate the relativistic cross section for Coulomb scattering, using our result from section 3.2. Eq. (84) applied to this example gives

$$\sigma = \mathcal{F} \int \frac{d^3 \mathbf{p}'}{(2\pi)^3 (2E'_p)} \frac{d^3 \mathbf{k}'}{(2\pi)^3 (2E'_k)} |\overline{\mathcal{M}}|^2 (2\pi)^4 \delta^4 (p' + k' - p - k). \quad (87)$$

As this expression is Lorentz invariant, we are free to choose which frame to evaluate it in. This is an extremely powerful tool to evaluate these integrals, as a careful choice can lead to considerable simplifications. We will choose the centre-of-mass frame here so that $\mathbf{p} = -\mathbf{k}$. We can easily do the the \mathbf{k}' integration using three of the δ -functions to give

$$\sigma = \mathcal{F} \int \frac{d^3 \mathbf{p}'}{(2\pi)^3} \frac{1}{4E'_p E'_k} |\overline{\mathcal{M}}|^2 (2\pi) \delta(E'_p + E'_k - E_p - E_k). \quad (88)$$

¹You can find a motivation for the flux factor in Aitchison and Hey and a more complete derivation in Peskin and Schröder chapter 4.5.

We will proceed by transforming to spherical polar coordinates, $d^3\mathbf{p}' = |\mathbf{p}'|^2 d|\mathbf{p}'| d\Omega$, where we have written the solid angle, $\sin\theta d\theta d\phi$, as $d\Omega$:

$$\sigma = \frac{\mathcal{F}}{(2\pi)^2} \int d\Omega d|\mathbf{p}'| \frac{|\mathbf{p}'|^2}{4E'_p E'_k} \overline{|\mathcal{M}|}^2 \delta(E'_p + E'_k - E_p - E_k). \quad (89)$$

We now make the change of variable $|\mathbf{p}'| \rightarrow E = E'_p + E'_k$, which has Jacobian factor

$$\frac{\partial E}{\partial |\mathbf{p}'|} = \frac{E|\mathbf{p}'|}{E'_p E'_k} \quad (90)$$

to get

$$\sigma = \frac{\mathcal{F}}{(2\pi)^2} \int d\Omega dE \frac{|\mathbf{p}'|}{4E} \overline{|\mathcal{M}|}^2 \delta(E - \sqrt{s}) = \frac{\mathcal{F}}{(2\pi)^2} \int d\Omega \frac{|\mathbf{p}'|}{4\sqrt{s}} \overline{|\mathcal{M}|}^2, \quad (91)$$

where it is understood that $\mathbf{k}' = -\mathbf{p}'$ with $|\mathbf{p}'|$ determined from $E = \sqrt{s}$. The only undefined variables are the angles which remain to be integrated over. We could now substitute the expression for $\overline{|\mathcal{M}|}^2$ explicitly in terms of these angles but it is actually informative to instead study the differential cross section

$$\frac{d\sigma}{d\Omega} = \frac{\mathcal{F}}{16\pi^2} \frac{|\mathbf{p}'|}{\sqrt{s}} \overline{|\mathcal{M}|}^2. \quad (92)$$

We will now consider the high energy limit where $s \gg m_e^2, m_\mu^2$. In this limit, the three Mandelstam invariants are given by

$$s = 4\mathbf{p}^2, \quad t = -4\mathbf{p}^2 \sin^2(\theta/2), \quad u = -4\mathbf{p}^2 \cos^2(\theta/2), \quad (93)$$

which gives

$$\overline{|\mathcal{M}|}^2 \simeq 2e^4 \frac{s^2 + u^2}{t^2} = \frac{2e^4}{\sin^4(\theta/2)} \left(1 + \cos^4 \frac{\theta}{2}\right). \quad (94)$$

Note that this amplitude squared has no dependence on the azimuthal angle ϕ . Using the conventional notation $\alpha = e^2/(4\pi)$, we obtain

$$\frac{d\sigma}{d\Omega} \simeq \frac{\alpha^2}{2s} \frac{1 + \cos^4(\theta/2)}{\sin^4(\theta/2)}. \quad (95)$$

4.3 The Coulomb Potential

The same calculation may be used to calculate the cross section for the scattering of a relativistic particle from an external Coulomb potential by working in the rest frame of the muon and taking $m_\mu \rightarrow \infty$. This is illustrated in fig. 6.

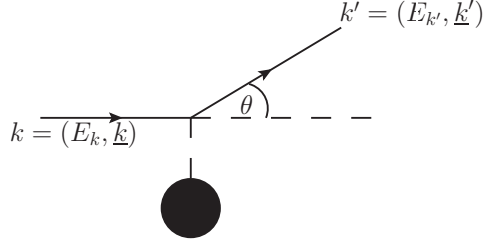


Figure 6: Scattering by an external Coulomb potential.

Repeating the same calculation in this limit yields

$$\begin{aligned} \frac{d\sigma}{d\Omega} &= \frac{\alpha^2}{4\mathbf{k}^2 \mathbf{v}^2 \sin^4(\theta/2)} (1 - \mathbf{v}^2 \sin^2(\theta/2)) \\ &= \left(\frac{d\sigma}{d\Omega} \right)_R (1 - \mathbf{v}^2 \sin^2(\theta/2)) , \end{aligned} \quad (96)$$

where $\mathbf{v} = |\mathbf{k}|/E_k$ and

$$\left(\frac{d\sigma}{d\Omega} \right)_R = \frac{\alpha^2}{4\mathbf{k}^2 \mathbf{v}^2 \sin^4(\theta/2)} \quad (97)$$

is the Rutherford cross section which was calculated in preschool problem 9. The extra \mathbf{v}^2 -term in eq. (96) then gives the relativistic correction to this. This result is entirely due to the electron being a spin-1/2 particle. If it were spin-0 instead, $|\overline{\mathcal{M}}|^2$ would look much simpler as there are no fermion traces to be performed and in that case we would find that there is no relativistic correction.

4.4 e^+e^- Annihilation

The calculation we have just performed is almost identical to $e^+(p') e^-(p) \rightarrow \mu^+(k) \mu^-(k')$. Although this now involves anti-particles, there is still one single diagram at leading-order and the trace algebra is very similar. Indeed we can re-interpret the incoming e^+ as an outgoing e^- with momentum $-p'$, and the outgoing μ^+ as an incoming μ^- with momentum $-k$. Then we do find explicitly that

$$\overline{|\mathcal{M}_{e^+(p')e^-(p) \rightarrow \mu^+(k)\mu^-(k')}|^2} = \overline{|\mathcal{M}_{e^-(p)\mu^-(-k) \rightarrow e^-(-p')\mu^-(k')}|^2} . \quad (98)$$

This is an example of “crossing symmetry”. Note in general that there is an additional minus sign for each fermion which swaps from the initial to final state or vice versa. This is because, for example,

$$\sum_r u_r(p') \bar{u}_r(p') = \not{p}' + m \longrightarrow \sum_r v_r(-p') \bar{v}_r(-p') = -\not{p}' - m = -(\not{p}' + m) . \quad (99)$$

In this case there are two minus signs whose combined effect gives just one.

If in e^+e^- -annihilation we take the approximation $m_e = 0$, we find

$$|\overline{\mathcal{M}}|^2 = \frac{8e^4}{s^2} [(pk)^2 + (pk')^2 + m_\mu^2(kk)'] , \quad (100)$$

Once again, choosing to work in the centre-of-mass frame, we find

$$\left(\frac{d\sigma}{d\Omega}\right)_{e^+e^- \rightarrow \mu^+\mu^-} = \frac{\alpha^2}{4s} \sqrt{1 - \frac{4m_\mu^2}{s}} \left(1 + \frac{4m_\mu^2}{s} + \left(1 - \frac{4m_\mu^2}{s}\right) \cos^2 \theta\right) . \quad (101)$$

If we again take the high-energy limit where $s \gg m_\mu^2$, this reduces to

$$\left(\frac{d\sigma}{d\Omega}\right)_{e^+e^- \rightarrow \mu^+\mu^-} = \frac{\alpha^2}{4s} (1 + \cos^2 \theta) . \quad (102)$$

We can now convert the above result to a total cross section by performing the integral over the solid angle. This gives

$$\sigma(e^+e^- \rightarrow \mu^+\mu^-) \simeq \frac{4\pi\alpha^2}{3s} . \quad (103)$$

Now, when an electron and positron annihilate, other fermions may be produced. If these are quarks, they are then observed in the detector as hadrons. The same calculation gives

$$\sigma(e^+e^- \rightarrow \text{hadrons}) = \frac{4\pi\alpha^2}{3s} N_c \sum_{i=1}^{n_f} Q_i^2 , \quad (104)$$

plus higher-order corrections, where there are N_c colours in each of the n_f massless flavours of quarks with charge Q_i . Therefore the ratio

$$R = \frac{\sigma(e^+e^- \rightarrow \mu^+\mu^-)}{\sigma(e^+e^- \rightarrow \text{hadrons})} \quad (105)$$

has been used to measure the number of colours to be $N_c = 3$.

5 Photon Scattering

In this section we will calculate the scattering amplitude for $e\gamma \rightarrow e\gamma$. In order to do that we need first to consider how to treat incoming and outgoing photons.

5.1 Photon Polarisation

We seek to find a plane-wave solution corresponding to a free photon (like our treatment for Dirac particles in section 2.1). It will have the form

$$A^\mu(x) = \varepsilon^\mu(k) e^{-ik \cdot x} , \quad (106)$$

where $\varepsilon^\mu(k)$ is the polarisation vector of the photon. In the Lorentz gauge of eq. (61), the photon equation of motion in eq. (51) is

$$\square A^\mu = 0, \quad (107)$$

and is automatically satisfied by a solution of the form in eq. (106), provided $k^2 = 0$. The Lorentz gauge condition gives an additional constraint on the polarisation vector

$$k \cdot \varepsilon(k) = 0. \quad (108)$$

However, there is still freedom here because, given a polarisation vector ε which solves this equation, any other vector of the form $\varepsilon' = \varepsilon + \lambda k$ will also be a solution, which corresponds to the propagation of an extra unphysical longitudinal photon, with a polarisation proportional to k_μ . This freedom is usually used to set $\varepsilon^0 = 0$ such that $\mathbf{k} \cdot \boldsymbol{\varepsilon} = 0$ so that the two physical polarisations ε^α , with $\alpha = 1, 2$, are in the transverse direction, and are chosen to be orthonormal. A useful relation we will use in the following is

$$\sum_{\alpha=1}^2 \varepsilon^{\alpha i}(k) \varepsilon^{\alpha j}(k) = \delta^{ij} - \hat{k}^i \hat{k}^j, \quad \text{where} \quad \hat{k}^i = \frac{k^i}{|\mathbf{k}|} = \frac{k^i}{k^0}. \quad (109)$$

The Feynman rule for an incoming photon is simply $\varepsilon^\mu(k)$ while for an outgoing photon it is $\varepsilon^{*\mu}(k)$, as shown in Fig. 4.

As for fermion spins, for unpolarised processes you compute the total cross section by averaging over incoming polarisations and summing over outgoing polarisations. Let us consider the case of a general process with one external incoming photon. The matrix element would have the form

$$i\mathcal{M} = \mathcal{A}^\mu \varepsilon_\mu(k). \quad (110)$$

The left-hand side is a physical quantity, hence it should give the same result for any choice of the gauge. Had we chosen $\varepsilon + \lambda k$ instead, this implies that $\mathcal{A}^\mu k_\mu$ has to vanish. This is a ‘‘Ward Identity’’ for QED, and is therefore a test of gauge-invariance.

Squaring the scattering-amplitude over the physical polarisations gives

$$\begin{aligned} \sum_{\alpha=1}^2 |\mathcal{A}^\mu \varepsilon_\mu^\alpha(k)|^2 &= \sum_{\alpha=1}^2 \mathcal{A}^\mu \mathcal{A}^{*\nu} \varepsilon_\mu^\alpha(k) \varepsilon_\nu^{*\alpha}(k) \\ &= A^i A^j (\delta^{ij} - \hat{k}^i \hat{k}^j), \end{aligned} \quad (111)$$

using eq. (109). The equation $\mathcal{A}^\mu k_\mu = 0$ implies $A^i \hat{k}^i = A^0$ and hence

$$\sum_{\alpha=1}^2 |\mathcal{A}^\mu \varepsilon_\mu^\alpha(k)|^2 = A^i A^i - A^0 A^0 = -A^\mu A^\nu g_{\mu\nu}. \quad (112)$$



Figure 7: The two tree-level diagrams for $e(p) \gamma(k) \rightarrow e(p') \gamma(k')$.

This could be done for each photon in turn if there were more in the process, and we find the general result that

$$\sum_{\alpha=1}^2 \varepsilon_{\mu}^{\alpha} \varepsilon_{\nu}^{*\alpha} \rightarrow -g_{\mu\nu}. \quad (113)$$

We have used the \rightarrow notation of Peskin and Schröder here as the result is not an exact equality in the absence of the rest of the matrix element, but the result is nonetheless true in any practical calculation.

5.2 Compton Scattering

There are two diagrams at leading order for this process, shown in Fig. 7. Following the Feynman rules in Fig. 4 and the rules for external photons in the previous subsection, we find that the sum of the two diagrams gives

$$i\mathcal{M} = -ie^2 \varepsilon^{*\mu}(k') \varepsilon^{\nu}(k) \bar{u}(p') \left(\gamma_{\mu} \frac{\not{p} + \not{k} + m}{(p+k)^2 - m^2} \gamma_{\nu} + \gamma_{\nu} \frac{\not{p} - \not{k}' + m}{(p-k')^2 - m^2} \gamma_{\mu} \right) u(p). \quad (114)$$

You can check explicitly that the above amplitude does indeed satisfy the appropriate QED Ward Identities, i.e. replacing $\varepsilon^{\nu}(k)$ with k^{ν} gives $\mathcal{M} = 0$, and similarly when replacing $\varepsilon^{*\mu}(k')$ with k'^{μ} (see tutorial sheet).

We now square the amplitude to get

$$\begin{aligned} |\overline{\mathcal{M}}|^2 &= \frac{1}{2} \sum_{\gamma \text{ pol}} \frac{1}{2} \sum_{e \text{ spin}} |\mathcal{M}|^2 \\ &= 2e^4 \left(\frac{(pk)}{(pk')} + \frac{(pk')}{(pk)} + 2m^2 \left(\frac{1}{(pk)} - \frac{1}{(pk')} \right) + m^4 \left(\frac{1}{(pk)} - \frac{1}{(pk')} \right)^2 \right). \end{aligned} \quad (115)$$

The calculation of the spin traces in this case requires the identities

$$\gamma_{\mu} \gamma^{\mu} = 4, \quad \gamma_{\mu} \gamma^{\rho} \gamma^{\mu} = -2\gamma^{\rho}, \quad (116)$$

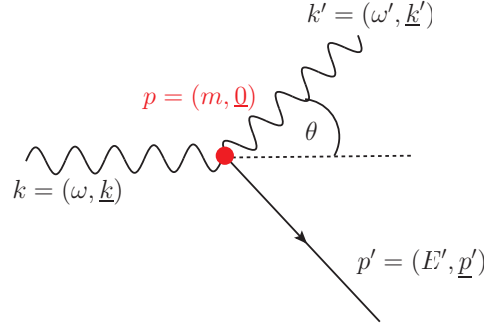


Figure 8: The Compton scattering process in the rest frame of the incoming electron.

from the problem sheet. We will again choose a suitable reference frame to simplify the calculation. In this case, it is convenient to work in the rest frame of the incoming electron as shown in fig. 8. We can use energy conservation to compute ω' :

$$\begin{aligned} m^2 = p'^2 &= (p + k - k')^2 = m^2 + 2m(\omega - \omega') - 2\omega\omega'(1 - \cos\theta) \\ \Rightarrow \omega' &= \frac{\omega}{1 + (\omega/m)(1 - \cos\theta)}. \end{aligned} \quad (117)$$

In this frame, we therefore have

$$|\overline{\mathcal{M}}|^2 = 2e^4 \left(\frac{\omega}{\omega'} + \frac{\omega'}{\omega} - \sin^2\theta \right). \quad (118)$$

The explicit dependence on the electron mass cancels with the factors of m in ω' . It is however present in the flux factor $\mathcal{F} = 1/(4m\omega)$. We now compute the integral over the phase space to get

$$\sigma = \frac{1}{4m\omega} \int \frac{d^3\mathbf{p}'}{(2\pi)^3(2E')} \frac{d^3\mathbf{k}'}{(2\pi)^3(2\omega')} 2e^4 \left(\frac{\omega}{\omega'} + \frac{\omega'}{\omega} - \sin^2\theta \right) (2\pi)^4 \delta^4(p' + k' - p - k). \quad (119)$$

We can again do the integral over $d^3\mathbf{k}'$ using the spatial parts of the δ -function. Then we transfer to spherical polars and find

$$\frac{d\sigma}{d\Omega} = \frac{\alpha^2}{2m^2} \left(\frac{\omega'}{\omega} \right)^2 \left(\frac{\omega}{\omega'} + \frac{\omega'}{\omega} - \sin^2\theta \right). \quad (120)$$

A nice check of this result is to take the low-energy limit where $\omega \ll m$. Then $\omega \simeq \omega'$ and we find

$$\frac{d\sigma}{d\Omega} = \frac{\alpha^2}{2m^2} (1 + \cos^2\theta). \quad (121)$$

This is the Thomson cross section for the scattering of classical electromagnetic radiation by a free electron. In the other limit, the high-energy limit where $\omega \gg m$, we have

$$\omega' \simeq \frac{m}{1 - \cos\theta} \quad \Rightarrow \quad \frac{d\sigma}{d\Omega} \simeq \frac{\alpha^2}{2m\omega} \frac{1}{1 - \cos\theta}. \quad (122)$$

and the cross section is strongly peaked for small angles. This leads to a logarithmic enhancement when you perform the angular integration. These “collinear” logarithms arise whenever massless particles are emitted; this will be discussed in more detail in the phenomenology course.

Note that, since $\omega > \omega'$, eq. (122) holds strictly for $(1 - \cos \theta) > m/\omega$. For smaller angles, eq. (121) holds and

$$\frac{d\sigma}{d\Omega} \simeq \frac{\alpha^2}{m^2}. \quad (123)$$

The forward (small scattering angle) Compton scattering cross section is then a valuable method to measure the QED coupling α .

6 Strong Interactions

In this section we will develop the theory of the strong interactions, quantum chromodynamics (QCD). The major difference between QED and QCD is that the gluons are self-interacting because they also carry colour charge (unlike the charge-neutral photon).

6.1 QCD Lagrangian

The particles which carry colour charge are

Spin-1/2: six families of quarks (up, charge and top with electric charge +2/3; down, strange and bottom with electric charge -1/3)
For each flavour, there are $N_c = 3$ of these.

Spin-1: $8 = (N_c^2 - 1)$ massless gluons.

The QCD Lagrangian for a quark of mass m is

$$\begin{aligned} \mathcal{L}_{\text{QCD}} &= -\frac{1}{4}F^{a\mu\nu}F_{\mu\nu}^a + \bar{\psi}_i(i\not{D}_{ij} - m\delta_{ij})\psi_j, \\ \text{with } D_{ij}^\mu &= \partial^\mu\delta_{ij} + ig_s t_{ij}^a A^{a\mu}, \quad F_{\mu\nu}^a = \partial_\mu A_\nu^a - \partial_\nu A_\mu^a + g_s f^{abc} A_\mu^b A_\nu^c. \end{aligned} \quad (124)$$

The a , i and j indices are gauge group indices which are discussed further below. The sum over these is implicit in eq. (124). Each t^a is a 3×3 matrix in colour space. The t^a matrices do not commute with each other, but obey the following algebra

$$[t^a, t^b] = if^{abc}t^c, \quad (125)$$

which is reminiscent of the algebra of angular momentum operators, $[J_i, J_j] = i\varepsilon_{ijk}J_k$. Here, in place of the alternating tensor ε_{ijk} , we have the “structure constants” f^{abc} (which also appear in $F_{\mu\nu}^a$). These are also completely anti-symmetric under the swapping of any pair of indices.

Just as the J_i generate the rotation group, $SU(2)$, the t^a generate the colour symmetry group, $SU(3)$. We choose to take the Pauli matrices as a representation of $SU(2)$. For $SU(3)$ we choose to take the representation where $t^a = \frac{1}{2}\lambda^a$ and the λ^a are the Gell-Mann matrices:

$$\begin{aligned} \lambda^1 &= \begin{pmatrix} 0 & 1 & 0 \\ 1 & 0 & 0 \\ 0 & 0 & 0 \end{pmatrix}, & \lambda^2 &= \begin{pmatrix} 0 & -i & 0 \\ i & 0 & 0 \\ 0 & 0 & 0 \end{pmatrix}, & \lambda^3 &= \begin{pmatrix} 1 & 0 & 0 \\ 0 & -1 & 0 \\ 0 & 0 & 0 \end{pmatrix}, \\ \lambda^4 &= \begin{pmatrix} 0 & 0 & 1 \\ 0 & 0 & 0 \\ 1 & 0 & 0 \end{pmatrix}, & \lambda^5 &= \begin{pmatrix} 0 & 0 & -i \\ 0 & 0 & 0 \\ i & 0 & 0 \end{pmatrix}, & \lambda^6 &= \begin{pmatrix} 0 & 0 & 0 \\ 0 & 0 & 1 \\ 0 & 1 & 0 \end{pmatrix}, \\ \lambda^7 &= \begin{pmatrix} 0 & 0 & 0 \\ 0 & 0 & -i \\ 0 & i & 0 \end{pmatrix}, & \lambda^8 &= \frac{1}{\sqrt{3}} \begin{pmatrix} 1 & 0 & 0 \\ 0 & 1 & 0 \\ 0 & 0 & -2 \end{pmatrix}. \end{aligned} \quad (126)$$

In practice, we are not interested in calculating one particular colour component and instead work with sums over all colours which ultimately leads to traces over the t^a -matrices. We will see explicit examples of this in the sections that follow and here just collect some useful identities:

$$\text{Tr}(t^a) = 0, \quad \text{Tr}(t^a t^b) = \frac{1}{2}\delta^{ab}, \quad \sum_a t_{ij}^a t_{jk}^a = C_F \delta_{ik}, \quad \sum_{a,b} f^{abc} f^{abd} = C_A \delta^{cd}, \quad (127)$$

where $C_F = \frac{4}{3}$, $C_A = 3$.

Notice that we have labelled with $a = 1, \dots, 8$ the gluon indices and with $i = 1, \dots, 3$ the quark indices. Particular care must be taken when these identities combine to give a trace of a δ -function:

$$\begin{aligned} \delta^{aa} &= N_c^2 - 1 = 8 \quad (\text{the number of gluons}) \\ \delta_{ii} &= N_c = 3 \quad (\text{the number of quarks}). \end{aligned} \quad (128)$$

The QCD Lagrangian \mathcal{L}_{QCD} is invariant under the infinitesimal ‘‘gauge’’ transformations

$$\begin{aligned} \psi_i(x) &\rightarrow (\delta_{ij} - ig_s \theta^a(x) t_{ij}^a) \psi(x), \\ A_\mu^a(x) &\rightarrow A_\mu^a(x) + D_\mu^{ab} \theta^b(x), \end{aligned} \quad (129)$$

where D_μ^{ab} is the covariant derivative in the ‘‘adjoint’’ representation, the one under which the gluon fields transforms under $SU(3)$, as opposed to the ‘‘fundamental’’ representation, which rules the transformation of quark fields. In particular, the adjoint covariant derivative is given by

$$D_\mu^{ab} = \partial_\mu \delta^{ab} + ig_s A_\mu^c (T^c)^{ab}, \quad (T^c)^{ab} = if^{acb} = -if^{abc}. \quad (130)$$

The matrices T^a , as needed for any generator of a representation of $SU(3)$, satisfy the same commutation rules as t^a :

$$[T^a, T^b] = if^{abc} T^c. \quad (131)$$

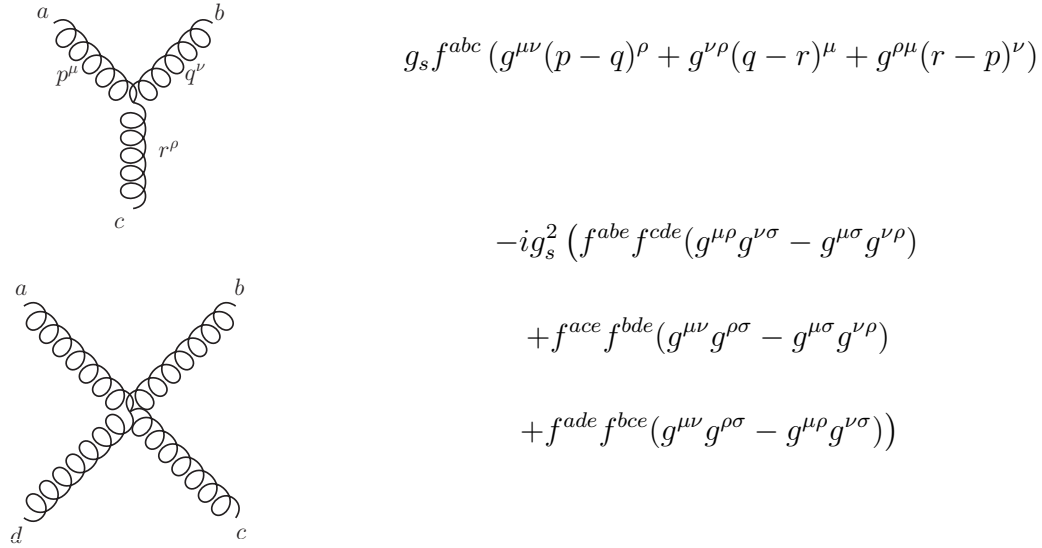


Figure 11: Three and four gluon vertices which arise from eq. (124). All momenta are taken to be incoming.

Returning to the Lagrangian, in QCD $F_{\mu\nu}^a$ has an extra term compared to QED, as required by gauge invariance. (Technically this term is present for QED too, but QED is an “Abelian” gauge theory which means that the structure constants are zero). Multiplying out $F^{a\mu\nu} F_{\mu\nu}^a$ give extra terms with 3 and 4 gauge fields. These correspond to new three- and four-gluon vertices as shown in fig. 11.

6.2 Gauge Invariance

The presence of the non-commuting colour matrices illustrates that $SU(3)$ is a non-Abelian gauge group. We can see the effect of this by studying the QCD equivalent of photon pair production, $q(p) \bar{q}(p') \rightarrow g(k) g(k')$, shown in fig. 12. In QED, the matrix element squared

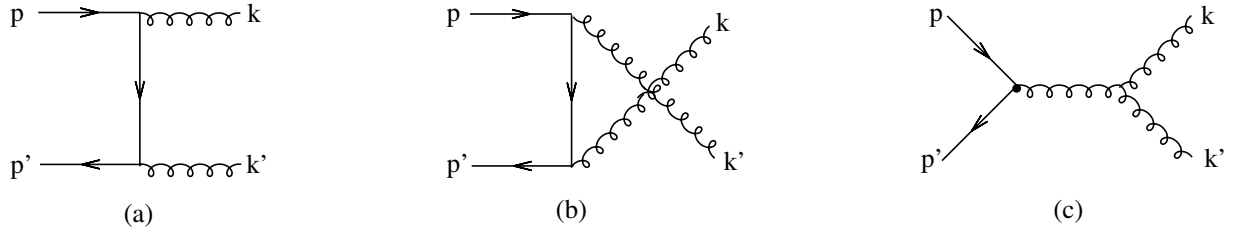


Figure 12: Feynman diagrams for the process $q\bar{q} \rightarrow gg$.

for this process can be obtained from that of Compton scattering via crossing.

One immediate effect is obvious – there is now a third diagram including the three-gluon

vertex. If we sum the contributions from the first two diagrams we find

$$\begin{aligned}\mathcal{M}^{(a)+(b)} &= \mathcal{A}_{\mu\nu}^{(a)+(b)} \varepsilon^{*\mu}(k) \varepsilon'^{\nu}(k'), \\ \mathcal{A}_{\mu\nu}^{(a)+(b)} &= -ig_s^2 \bar{v}(p') \left(\gamma_\nu t^b \frac{\not{p} - \not{k}}{(p-k)^2} \gamma_\mu t^a + \gamma_\mu t^a \frac{\not{p} - \not{k}'}{(p-k')^2} \gamma_\nu t^b \right) u(p),\end{aligned}\tag{135}$$

where we have implicitly assumed that gluon k has colour a and polarisation index μ , and gluon k' has colour b and polarisation index ν . At this order, see eq. (133), gauge invariance corresponds to testing whether the replacement $\epsilon_\mu \rightarrow \epsilon_\mu + \lambda k_\mu$ leaves the amplitude invariant. This is equivalent to testing the condition for the Ward Identity, $\mathcal{A}_{\mu\nu}^{(a)+(b)} k^\mu = 0$:

$$\mathcal{A}_{\mu\nu}^{(a)+(b)} k^\mu = -ig_s^2 [t^a, t^b] \bar{v}(p') \gamma_\nu u(p) \neq 0.\tag{136}$$

The non-zero commutator makes these diagrams alone not gauge-invariant. Adding diagram (c) gives a contribution which exactly cancels this (try this!) but yields another term proportional to k'_μ . This vanishes when we remember the whole expression is contracted with $\varepsilon'^{\nu}(k')$, and so gauge invariance is only obeyed once we project onto physical polarisations. This wasn't necessary in QED.

Recall in the QED case in section 3.2, we used $\mathcal{A}_{\mu\nu} k^\mu = 0$ to show that, in practical calculations, we can always make the replacement

$$\sum_{\alpha=1}^2 \varepsilon_\mu^\alpha \varepsilon_\nu^{*\alpha} \rightarrow -g_{\mu\nu}.\tag{137}$$

Although the right-hand summed all polarisations and not only the physical transverse ones, in actual calculations the unphysical longitudinal gluon polarisations automatically cancelled. This is no longer the case in QCD, where one has to sum strictly over physical polarisations. However, this can make calculations more cumbersome, so it might still be useful to sum over all polarisations, and to cancel in some way the unphysical degrees of freedom. How this cancellation is performed depends on the gauge. In covariant gauges, like the Feynman gauge, this is done by introducing extra fields, called the ghost fields. The alternative is to use the so-called physical gauges, that ensure that that only physical degrees of freedom propagate on shell.

Ghost Fields

To understand how the cancellation of unphysical polarisations actually arises in a covariant gauge, we need to revert to the case of photon pair production in QED. When we make the replacement in eq. (137), we are exploiting the fact that QED is unitary, i.e. probability is conserved through time evolution. A non-trivial implication of unitarity is that, at the lowest order in perturbation theory, twice the imaginary part of the forward amplitude for the process $e^+e^- \rightarrow e^+e^-$ has to be equal to amplitude squared for the process $e^+e^- \rightarrow \gamma\gamma$, when we integrate over the photon phase space and sum over *physical* photon polarisations. This is illustrated in Fig. 13, which shows the only intermediate

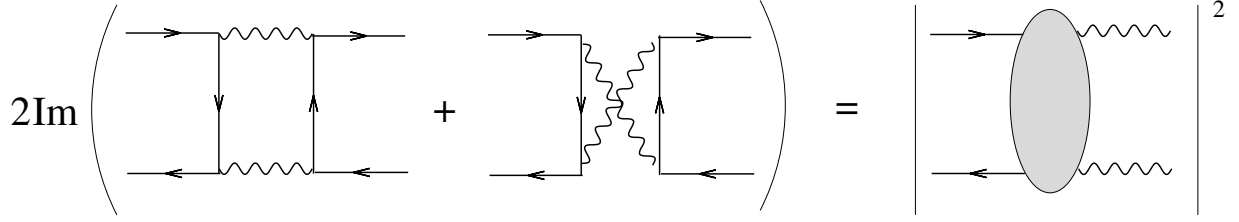


Figure 13: Unitarity relation for the process $e^+e^- \rightarrow \gamma\gamma$. The shaded blob represent the sum of all possible subdiagrams that can give rise to two photons in the final state at the lowest order in perturbation theory.

states that, at the considered order in perturbation theory, give a non-zero imaginary part, namely two virtual photons. Furthermore, it is possible to show that the imaginary part of any Feynman diagram is obtained by putting on shell in all possible ways the intermediate propagators (i.e. cutting the diagram) by replacing $i/(p^2 - m^2 + i\varepsilon)$ in each of them by $(2\pi)\Theta(p_0)\delta(p^2 - m^2)$. This divides each Feynman diagram into two subdiagrams on either side of the cut. On one side of the cut, one uses standard Feynman rules. On the other sides, one needs to apply complex conjugation to all Feynman vertices and propagators. Cuts of a diagram that conflict with energy-momentum conservation do not give any contribution to the imaginary part. The result of this cutting procedure for the present case is illustrated in Fig. 14. The dashed line on the right-hand side of the figure represents the only cut of the diagram that gives a non-zero imaginary part, obtained by putting on shell the intermediate photon propagators. If the amplitude is computed in the Feynman

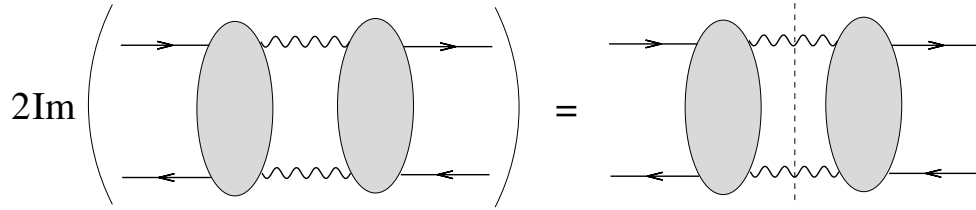


Figure 14: Pictorial representation of the cutting rules needed to compute the imaginary part of the forward amplitude $e^+e^- \rightarrow e^+e^-$ mediated by two virtual photons. The shaded blob represents the sum all possible subdiagrams that can give two photons in the intermediate state, that is, the two diagrams on the left-hand side of Fig. 13.

gauge, for an intermediate photon of momentum k , we have to perform the replacement

$$-g_{\mu\mu'} \frac{i}{k^2 + i\varepsilon} \rightarrow -g_{\mu\mu'} (2\pi)\Theta(k_0)\delta(k^2). \quad (138)$$

Let us call $A^{\mu\nu}$ the contribution to the diagram on the left of the cut in Fig. 14. From the Ward identity $k_\mu A^{\mu\nu} = 0$, we obtain that the contribution of gluon k to the imaginary part of the amplitude becomes

$$\int \frac{d^4k}{(2\pi)^4} (-g_{\mu\mu'}) (2\pi)\Theta(k_0)\delta(k^2) A^{\mu\nu} = \int \frac{d^3k}{(2\pi)^3 2k_0} A^{\mu\nu} \sum_{\alpha=1}^2 \epsilon_\mu^\alpha(k) \epsilon_{\mu'}^{*\alpha}(k), \quad (139)$$

where $\alpha = 1, 2$ is the index labelling photon physical polarisations. This verifies explicitly the unitary relation represented in Fig. 13. The latter means that, in QED, making the replacement in eq. (137) corresponds to exploiting the unitarity of the theory to compute an amplitude squared through the imaginary part of the corresponding forward amplitude.

In the case of QCD, as we have seen in the previous section, the fact that $k_\mu \mathcal{A}^{\mu\nu} \neq 0$ implies that the amplitude squared for the process $q\bar{q} \rightarrow gg$ is not given by the imaginary part of the forward amplitude $q\bar{q} \rightarrow q\bar{q}$, when only gluons are considered as intermediate states. In fact, the cut forward amplitude contains the contribution of non-physical longitudinal polarisations, which do not contribute to the amplitude squared for $q\bar{q} \rightarrow gg$. This would violate unitarity, so there has to be additional fields that are responsible for the cancellation of the contribution of non-physical polarisations in the imaginary part of the forward amplitude. These new fields are called ghosts. They are scalar fields, but satisfy Pauli exclusion principle like fermions. They transform under $SU(3)$ in the same way as gluons, i.e. in the adjoint representation. The Feynman rules for ghosts are shown in fig. 15. They can propagate and couple to gluons, but never appear in physical final states. If

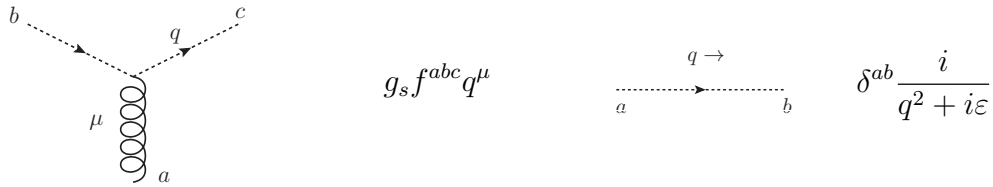


Figure 15: The Feynman rules for ghost fields, which are constructed explicitly to cancel unphysical degrees of freedom.

we now consider the imaginary part of the forward $q\bar{q}$ amplitude, at the lowest order in perturbation theory we need to include not only gluons as intermediate states, but ghosts as well, as pictorially illustrated in Fig. 16. The ghost-antighost loop contributes to the imaginary part of the forward amplitude with a factor (-1) , just like a normal fermion loop, so as to cancel the contribution of the unphysical longitudinal gluon polarisations when summing over all diagrams. The resulting imaginary part equals the amplitude squared for the process $q\bar{q} \rightarrow gg$, integrated over the gluon phase space and summed over physical gluon polarisations, as required by unitarity of QCD.

Physical Gauges

Alternatively, we can impose a so-called “physical gauge” condition on the gluon fields to eliminate unphysical polarisations from the start. This eliminates the need for ghosts, which do not interact with gluons anymore, but complicates the gluon propagator. In place of the Lorentz gauge condition $\partial^\mu A_\mu^a = 0$, we impose

$$A_\mu^a n^\mu = 0, \quad (140)$$

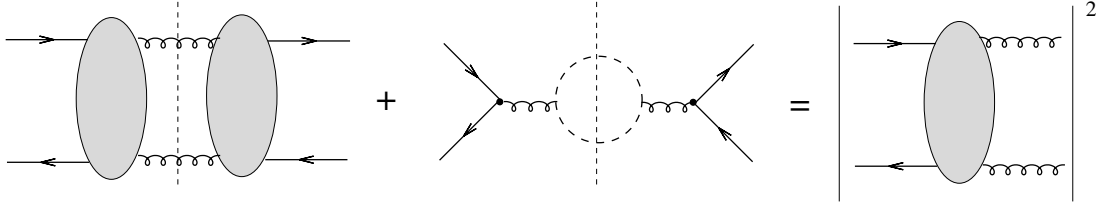


Figure 16: Pictorial representation of the unitarity constraint for QCD discussed in the text. Longitudinal polarisations for on-shell gluons in the cut amplitude on the left-hand side of the equality are cancelled by the contribution of the ghost-antighost loop. Each blob represents the sum of the three diagrams in Fig. 12.

for some arbitrary reference vector n^μ . This is done by adding the gauge-fixing Lagrangian

$$\mathcal{L}_{\text{gf}} = -\frac{1}{2\xi}(A_\mu^a n^\mu)^2, \quad (141)$$

and taking the limit $\xi \rightarrow 0$, thus enforcing the gauge condition in eq. (140).

The new expression for the propagator (for $\xi = 0$) is shown in fig. 17. When we use a

$$\overset{\mu}{\underbrace{\text{oooooo}}_a} \xrightarrow{q} \overset{\nu}{\text{oooooo}}_b \quad \delta^{ab} \frac{i}{q^2 + i\varepsilon} \left(-g^{\mu\nu} + \frac{q^\mu n^\nu + q^\nu n^\mu}{(qn)} - n^2 \frac{q^\mu q^\nu}{(qn)^2} \right)$$

Figure 17: The gluon propagator when working in a physical gauge, $A_\mu^a n^\mu = 0$.

physical gauge, whenever we sum over polarisations, we can make the replacement

$$\sum_{\alpha=1}^2 \varepsilon_\mu^\alpha(q) \varepsilon_\nu^{*\alpha}(q) \rightarrow -g_{\mu\nu} + \frac{q^\mu n^\nu + q^\nu n^\mu}{(qn)} - n^2 \frac{q^\mu q^\nu}{(qn)^2}. \quad (142)$$

The different choices of reference vector n^μ correspond to different choices of the gauge. One can explicitly check that results for physical quantities, such as cross sections, are independent of this choice.

A relevant example of a physical gauge is the light-cone gauge, in which $n^2 = 0$. In such a gauge, if we have an on-shell gluon $q = (\omega, \mathbf{q})$, we can choose $n = (1, -\mathbf{q}/\omega)$. In this case

$$-g_{\mu\nu} + \frac{q^\mu n^\nu + q^\nu n^\mu}{(qn)} = \sum_{\alpha=1}^2 \varepsilon_\mu^\alpha(q) \varepsilon_\nu^{*\alpha}(q), \quad (143)$$

so that the replacement gives exactly the sum over the physical polarisations introduced in section 5.1. The expression in eq. (143) is the one that must be used in covariant gauges if one does not want to introduce unphysical amplitudes squared with ghosts in the final state.



Figure 18: Sample “loop” Feynman diagrams: (a) one of the one-loop corrections to Coulomb scattering and (b) a one-loop correction to the photon propagator.

7 Renormalisation

7.1 Dimensional regularisation and renormalisation scale

As mentioned in section 3.2, starting from the Feynman rules one can construct diagrams with loops, as for example the diagrams shown in fig. 18. The presence of loops means that momentum-conservation at each interaction vertex is no longer sufficient to determine the momentum in each leg. For example, k can take any value in the diagrams shown in fig. 18. We must therefore integrate over all possible values of unconstrained loop momenta. For example, the result for the diagram in fig. 18(b) is

$$(ie)^2 \int \frac{d^d k}{(2\pi)^4} \frac{\text{Tr}[\gamma_\mu(\not{k} + \not{p} + m)\gamma_\nu(\not{k} + m)]}{(k^2 - m^2)((k + p)^2 - m^2)}, \quad (144)$$

with p the photon momentum and d the number of space-time dimensions. As the integral runs over all values of k , it includes very large values of k . Counting the powers of k , there are six of them in the numerator and four in the denominator, which implies that this integral diverges. In general, for any integral of the form

$$\int \frac{d^d k}{(2\pi)^4} \frac{N(k)}{M(k)} \quad (145)$$

we define the superficial degree of divergence, D , to be the result of the naïve power-counting:

$$D = d + (\text{powers of } k \text{ in } N) - (\text{powers of } k \text{ in } M). \quad (146)$$

If $D \geq 0$, then the integral is said to be superficially divergent. Such divergences are called ultra-violet (UV) because they arise whenever loop momenta get large. The boundary case of $D = 0$ is a logarithmic divergence (think of $\int dk 1/k$). The term “superficial” is used because there can be other factors which can affect the actual degree of divergence. In the example above, gauge invariance actually implies that the final result of the integral in eq. (144) must be proportional to $(p^2 g_{\mu\nu} - p_\mu p_\nu)$. Therefore the divergence is only logarithmic, and not quadratic as it appears from naïve power counting.

The main point, though, is not the degree of divergence, but the fact that one finds divergences at all. These higher-loop corrections were supposed to be corrections in the

perturbative series, hence smaller than those appearing at the previous perturbative order. For many years, this caused a major problem for the development of perturbation theory. However, there exists a well-defined procedure to “remove” these divergences which is called renormalisation. The basic idea behind renormalisation is that the parameters appearing in the Lagrangian do not need to be physical quantities, but their value is determined by comparing perturbative predictions to actual experimental data. For instance, the value of e can be extracted by measuring the Compton differential cross section at small angles. Therefore, infinities that eventually appear in perturbative calculations can be in principle reabsorbed in a redefinition of the parameters entering the Lagrangian. In practice, this amounts to rescaling all quantities in the Lagrangian by a “renormalisation constant”, Z . For instance, for a field ϕ we have

$$\phi \longrightarrow \phi_0 = Z_\phi \phi_R. \quad (147)$$

The field ϕ_0 is called “bare” field, as opposed to the “renormalised” field ϕ_R , and Z_ϕ is called renormalisation constant. This procedure has to be repeated for all fields, masses and coupling constants. Provided that *all* infinities in the theory can be removed with a finite number of renormalisation constants Z , then the theory is said to be renormalisable. After the renormalisation constants have been fixed, we can calculate all physical quantities in terms of the renormalised quantities and the results will be both finite and unambiguously defined.

The renormalisation constants are calculated according to some procedure that is called “renormalisation scheme”. This consists in computing a suitable set of correlation functions, and imposing that these functions are finite at any order in perturbation theory. In this procedure one finds divergent integrals, which have to be regularised in some way. The regularisation actually provide means to parameterise the divergence. One approach is to implement a momentum cut-off, Λ , so as to artificially remove the region with large momentum. The most common approach though is called “dimensional regularisation”. Here we decrease the term d in eq. (146) to a lower value, so that we calculate all integrals in $d = 4 - 2\epsilon$ dimensions instead of $d = 4$. The integration measure becomes

$$\frac{d^4 k}{(2\pi)^4} \longrightarrow \frac{d^{4-2\epsilon} k}{(2\pi)^{4-2\epsilon}}, \quad (148)$$

and for each dimensionless coupling g_R one performs the replacement

$$g_R \rightarrow \mu^{\frac{4-d}{2}} g_R(\mu) = \mu^\epsilon g_R(\mu). \quad (149)$$

The factor of μ^ϵ is essential to preserve the correct dimensions of the bare coupling in d dimensions. The renormalised coupling g_R stays dimensionless and depends now on the scale μ . The latter quantity is the famous renormalisation scale and it is the price that we pay for renormalisation as our finite calculations are now all dependent upon μ .

To summarise, the steps to perform renormalisation within dimensional regularisation are:

1. Compute all integrals in terms of renormalised quantities.

2. All UV divergences appear as $1/\epsilon$ -poles.
3. Define the renormalisation functions Z so as to cancel the poles in ϵ (and maybe some finite terms).

After renormalisation, eq. (147) depends on both ϵ and μ , as follows:

$$\phi_0(\epsilon) = Z_\phi(\mu, \epsilon) \phi_R(\mu), \quad (150)$$

and a similar expression holds for all couplings and masses. Both ϕ_0 and Z are infinite for $\epsilon \rightarrow 0$, whereas $\phi_R(\mu)$ stays finite, but depends on the unphysical renormalisation scale μ .

In a renormalised theory then, even tree-level diagrams depend on the renormalisation scale, through the coupling for example. The dependence on the renormalisation scale would disappear only if we were able to calculate physical quantities to all orders in perturbation theory. Although this is unpractical, calculating one or two extra orders in perturbation theory can reduce the dependence considerably. However, this does mean that any theoretical calculation now depends on a free parameter, and it is exactly this parameter which leads to a way to estimate the “theory uncertainty”. In fact, consider an observable $O(\alpha_R(\mu), \mu, \{Q_i\})$, where $\{Q_i\}$ is a set of characteristic scales for the process. If we know $O^{(n)}$, the perturbative expansion of O at order n in perturbation theory, we have

$$O^{(n)}(\alpha_R(\mu'), \mu', \{Q_i\}) = O^{(n)}(\alpha_R(\mu), \mu, \{Q_i\}) + \mathcal{O}(\alpha_R^{n+1}(\mu)), \quad (151)$$

so that the variation of μ around some central value μ_0 produces automatically a higher-order term. Notice that $O^{(n)}(\alpha_R(\mu), \mu, \{Q_i\})$ might contain $\ln(Q_i/\mu)$. This is why the central scale μ_0 is normally chosen of the order of the typical value that the scales Q_i can assume. For example in $gg \rightarrow H$, one would typically take $\mu_0 \sim m_H$.

The obvious way to gauge how the strength of the dependence on the scale in a calculation is to vary the scale and see how the result varies. If the dependence is very weak, the result will be negligible. If the dependence is very strong, the variation will be large. The consensus of the community is to quote the theoretical uncertainty when the central scale is varied by a factor of 2 in each direction. One should remember that this is only an uncertainty of the dependence on the renormalisation scale and not a strict error bar. This is illustrated by the plot in fig. 19, which is taken from Gehrmann-De Ridder, Gehrmann, Glover & Pires, arXiv:1301.7310. It shows the scale dependence for inclusive jet production in the gluon-gluon channel at LO, NLO and NNLO. Indeed the variation decreases each time indicating that the sensitivity to the scale is decreasing. The fact that the lines do not overlap is a clear sign that these uncertainty bands are not error bands.

7.2 Running Coupling

Suppose we have chosen a renormalisation scale μ . How do we measure a coupling $\alpha_R(\mu)$? We normally consider an observable $O(\alpha_R(\mu'), \mu', \{Q_i\})$, compute it at the highest possible

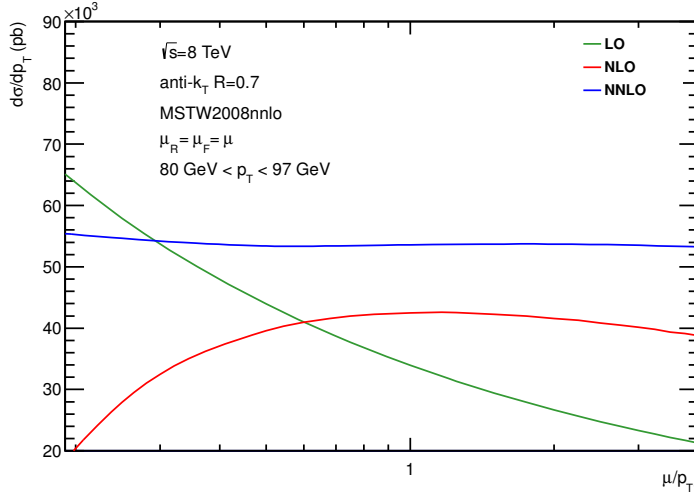


Figure 19: Plot showing the scale dependence for inclusive jet production at LO, NLO and NNLO, taken from Gehrmann-De Ridder, Gehrmann, Glover & Pires, arXiv:1301.7310.

order in perturbation theory, and compare the obtained number with experimental data:

$$O^{(n)}(\alpha_R(\mu'), \mu', \{Q_i\}) = O_{\text{exp}} \Rightarrow \alpha_R(\mu). \quad (152)$$

By doing this for various observables, characterised by different typical scales μ , one can actually measure the dependence of the coupling on the renormalisation scale μ . This dependence can be predicted theoretically, and the comparison of the predicted dependence with the one that is actually observed represents one of the most stringent tests of the validity of a given QFT. This is illustrated for QCD in fig. 20, where one sees an astonishing agreement between the predicted “running” of the QCD coupling with the renormalisation scale Q , and what is observed in experimental data.

The theoretical object that dictates how a coupling evolves with the renormalisation scale is the beta function $\beta(\alpha_R)$, defined as

$$\mu^2 \frac{\partial \alpha_R}{\partial \mu^2} = \beta(\alpha_R) = -\beta_0 \alpha_R^2 - \beta_1 \alpha_R^3 + \dots \quad (153)$$

There are various ways to compute the beta function, which in general depends on the renormalisation scheme used. However, one can show that the first two coefficient of the beta function, β_0 and β_1 , are independent of the renormalisation scheme. If we consider a scheme tied to dimensional regularisation (e.g. the so-called $\overline{\text{MS}}$ scheme), one has the relation

$$\alpha_0(\epsilon) = \mu^{2\epsilon} Z_g^2(\epsilon, \mu^2) \alpha_R(\mu^2), \quad (154)$$

where $\alpha_0 = g_0^2/(4\pi)$ and $\alpha_R = g_R^2/(4\pi)$. The crucial observation is that the bare coupling α_0 does not depend on μ . Therefore, its logarithmic derivative with respect to μ^2 is zero:

$$0 = \mu^2 \frac{\partial \alpha_0}{\partial \mu^2} = \mu^{2\epsilon} Z_g^2(\epsilon, \mu^2) \left[\left(\epsilon + \frac{\mu^2}{Z_g^2} \frac{\partial Z_g^2}{\partial \mu^2} \right) \alpha_R + \mu^2 \frac{\partial \alpha_R}{\partial \mu^2} \right]. \quad (155)$$

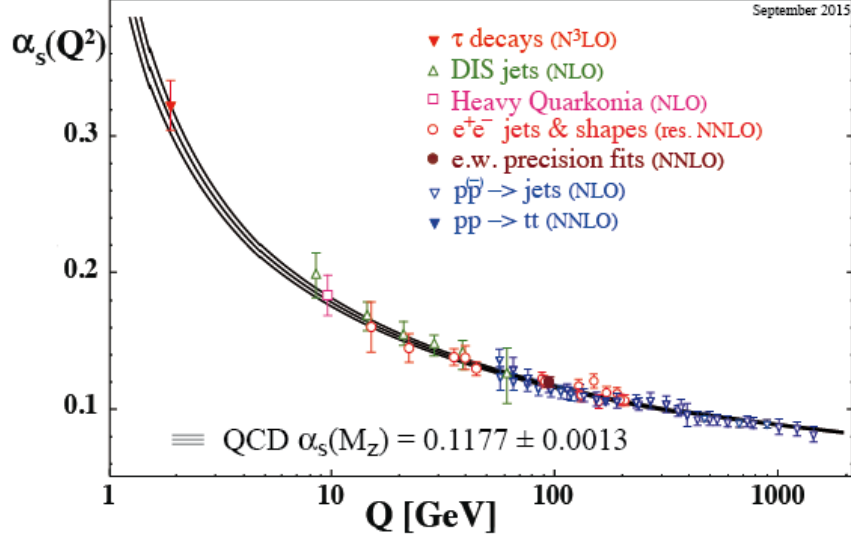


Figure 20: The QCD coupling α_s as a function of the renormalisation scale Q , in theory and experiment, taken from arXiv:1512.0519.

This gives

$$\mu^2 \frac{\partial \alpha_R}{\partial \mu^2} = - \left(\epsilon + \frac{\mu^2}{Z_g^2} \frac{\partial Z_g^2}{\partial \mu^2} \right) \alpha_R \equiv \beta(\epsilon, \alpha_R) \rightarrow \beta(\alpha_R) = - \lim_{\epsilon \rightarrow 0} \frac{\mu^2}{Z_g^2} \frac{\partial Z_g^2}{\partial \mu^2} \alpha_R, \quad \epsilon \rightarrow 0. \quad (156)$$

In any scheme based on dimensional regularisation we have

$$Z_g(\epsilon, \mu^2) = 1 + \frac{\alpha_R(\mu^2)}{\epsilon} Z_g^{(1)} + \dots \quad (157)$$

Therefore the first term of the beta function is just obtained from the $1/\epsilon$ pole of Z_g , as follows

$$\beta(\alpha_R) = - \lim_{\epsilon \rightarrow 0} \frac{\mu^2}{Z_g^2} \frac{\partial Z_g^2}{\partial \mu^2} \alpha_R = - \lim_{\epsilon \rightarrow 0} \frac{2Z_g^{(1)}}{\epsilon} \underbrace{\mu^2 \frac{\partial \alpha_R}{\partial \mu^2}}_{=-\epsilon \alpha_R} \alpha_R = -\beta_0 \alpha_R^2 \quad \Rightarrow \quad \beta_0 = -2Z_g^{(1)}. \quad (158)$$

The calculation of $Z_g^{(1)}$ can be performed using any quantity that involves an interaction vertex. A way that is common to both QED and QCD is to consider the renormalised interaction Lagrangian

$$\mathcal{L}_{\text{int}} \rightarrow Z_g Z_2 \sqrt{Z_3} (g_R \bar{\psi}_R \mathcal{A}_R \psi_R) = Z_1 (g_R \bar{\psi}_R \mathcal{A}_R \psi_R), \quad \Rightarrow \quad Z_g = \frac{Z_1}{Z_2 \sqrt{Z_3}}. \quad (159)$$

Here we have used the ubiquitous notation $Z_\psi = \sqrt{Z_2}$ and $Z_A = \sqrt{Z_3}$. The function Z_1 contains all UV divergences associated with loop corrections to the interaction vertex, whereas Z_2 and Z_3 contain UV divergences arising in the calculations of the fermion

and gauge-boson propagators respectively. In QED, a powerful Ward identity implies $Z_1 = Z_2$, so that the beta function can be calculated just from all the loop corrections to the propagator in the unrenormalised theory. For the case of QED

$$\beta_0 = -2Z_g^{(1)} = Z_3^{(1)} = -\frac{1}{3\pi}. \quad (160)$$

Inserting this expression in the beta function we obtain

$$\beta_{\text{QED}}(\alpha) = \frac{1}{3\pi}\alpha^2. \quad (161)$$

which means that the QED coupling, at least until the beta function is dominated by its first term, becomes stronger with energy.

In QCD instead the Ward identity $Z_1 = Z_2$ does not hold any more. However, it holds at least for the part of these renormalisation functions that depends on C_F . Since, at one loop, $Z_2^{(1)}$ is proportional to C_F , its contribution to the beta function cancels exactly with the abelian contribution to $Z_1^{(1)}$. Therefore, the only contributions to the QCD beta function at one loop come from the renormalisation function of the gluon $Z_3^{(1)}$ and the non-abelian part of $Z_1^{(1)}$, which we call $Z_1^{(1)}|_{\text{n.a.}}$. The two depend on the gauge, but this gauge dependence cancels in the combination

$$\beta_0 = -2Z_g^{(1)} = Z_3^{(1)} - 2Z_1^{(1)}|_{\text{n.a.}}. \quad (162)$$

For instance, in the Feynman gauge

$$Z_3^{(1)} = \frac{\alpha_s}{\epsilon} \frac{5C_A - 2n_f}{12\pi}, \quad Z_1^{(1)} = -\frac{\alpha_s}{\epsilon} \frac{C_F + C_A}{4\pi}, \quad (163)$$

where $\alpha_s = g_s^2/(4\pi)$ and n_f is the number of massless (a.k.a. “active”) quark flavours contributing to the renormalisation of the gluon propagator. This gives

$$\beta_{\text{QCD}}(\alpha_s) = -\frac{11C_A - 2n_f}{12\pi}\alpha_s^2 = -\frac{21}{12\pi}\alpha_s^2, \quad (164)$$

where the latter expression corresponds to the actual value of the beta function for $n_f = 6$ active flavours, as is the case at very high momentum scales. The fact that the beta function of QCD is negative when α_s is small means that the QCD coupling decreases with energy. This property is known as asymptotic freedom, and is crucial to be able to compute hadronic cross sections in terms of quarks and gluons. In fact, when probed at short distances, hadrons appear as made up of pointlike constituents, quarks and gluons, which interact very feebly. Therefore, the Feynman rules we have learnt so far are enough to compute high-energy observables, for instance jet cross sections, as will be explained in the phenomenology course. At larger distances, the QCD coupling becomes stronger and stronger, at a point that quarks and gluons bind together to form hadrons. This phenomenon is known as confinement.

Summary

This has been a very quick tour through some very important, deep and interesting material. I hope it has provided some insight into the quantum field theory descriptions of QED and QCD, and provided you with useful tools for the future.

Acknowledgements

It has been a pleasure to give this course at the 2016 HEP Summer School. I would like to thank Nikos Konstantinidis for directing this successful school, the other lecturers and tutors for making this such an interesting and entertaining fortnight, and the students for engaging with the courses.